Distance Dependence of Photoinduced Electron Transfer in Metalloporphyrin Dimers†

Carmita F. Portela,[‡,§] Jarmila Brunckova,[‡] Joseph L. Richards,[‡,||] Bernd Schöllhorn,[‡,⊥] Yassuko Iamamoto,[▽] Douglas Magde,[‡] Teddy G. Traylor,[‡,⊗] and Charles L. Perrin*[,‡]

Department of Chemistry and Biochemistry, University of California—San Diego, 9500 Gilman Drive, La Jolla, California 92093-0506, Universidade Federal de Pernambuco, Recife, Brazil, Universidade de São Paulo, Ribeirão Preto, Brazil

Received: June 2, 1999; In Final Form: September 7, 1999

To study the dynamics and mechanism of intramolecular photoinduced electron transfer (PET) reactions, a series of (Zn^{II}−Fe^{III}) *meso*-tetraarylmetalloporphyrin dimers were synthesized and the kinetics of their PET reactivity was measured. Molecular building blocks were prepared by selective nucleophilic aromatic substitution of a para fluorine on tetraarylporphyrins containing a single pentafluorophenyl group. This synthetic approach allows a wide variety of systematic modifications such as type and length of spacer, metal center, and redox-potential difference between donor and acceptor. The edge-to-edge distance between the two porphyrins varies from 14.4 to 27.3 Å. Into a symmetric dimer, with two identical porphyrins covalently linked by a rigid partly saturated bridge, one zinc(II) and one iron(III) can be inserted. From measurements of fluorescence lifetimes the rate constants for PET from the electronically excited state of the zinc porphyrin to the bis(imidazole)iron porphyrin cation were evaluated. The electron-transfer rate decreases by a factor of only 165 when the distance increases by 13 Å. This small decrease is indicative of a surprisingly weak attenuation of the electronic coupling with distance.

Introduction

Over the past decade substantial theoretical and experimental effort has been directed toward understanding the dynamics of electron transfer (ET) in both proteins and model compounds.[1] Remarkable progress has been achieved through experiments with defined distances, energetics, and orientations of electron donor and acceptor in supramolecules. Nevertheless, an incompletely solved problem is the delineation of the factors that control the dependence of ET rates on the distance between the electron donor and the electron acceptor.[2] A theoretical model has been developed for electron tunneling across proteins.[3] The distance dependence of ET across DNA is currently a matter of considerable controversy.[4]

Covalently linked porphyrin−quinone diads have been extensively studied from the point of view of photoinduced electron transfer (PET).[5−13] However, considerably less information is available for two porphyrins covalently linked by a rigid spacer.[14,15] McLendon and co-workers studied PET in a series of Zn,Fe protoporphyrin dimers where the bridge consists of either one, two, or three para-linked phenyl groups.[16] They found a weak distance dependence for the ET rates, which was interpreted in terms of a moderate loss of conjugation at each phenyl junction. This result can be described by a simple theory that assumes delocalization within the phenyl ring.

The molecular structure of the bridge plays an important role in ET between donor and acceptor moieties.[17] In most cases ET occurs through the bonds of the bridge and not through the surrounding medium. Often ET appears to be mediated by a superexchange mechanism involving the antibonding orbitals of the bridge.[18] Therefore, aromatic and unsaturated bridges are expected to be more effective than fully saturated bridges.

A recent study of three supramolecular porphyrin systems allowed a comparison of the electronic coupling provided by σ, π, and hydrogen bonds.[19] Contrary to general expectations, the electronic coupling across a hydrogen-bond interface is greater than that across an analogous interface composed entirely of carbon−carbon σ bonds. Moreover, only a two-fold increase in the ET rate was observed in a porphyrin dimer with a π-containing *cis*-bicyclo[3.3.0]octa-2,6-dien-3,7-ylidene (BCOE), as compared to the saturated *cis*-bicyclo[3.3.0]octan-3,7-ylidene (BCO) linker.

To test how the efficiency of ET is related to the molecular structure of the spacer, systems with rigid, nonaromatic bridges that impose a well-defined molecular geometry should be investigated. Through the precise experimental control of geometry, we hope to provide further experimental information for refinement of theoretical treatments. We now report the results of photoinduced ET in a series of metalloporphyrin dimers rigidly connected by systems including aliphatic rings. The saturated rings used here offer the advantages of high chemical stability and superior insulating characteristics, which we expect will minimize direct interactions between the donor and acceptor chromophores. The minimal interaction is important for analogy to photosynthetic reaction centers, where the key chromophores are separated by large distances.

The development of a method[20] for the preparation of functionalized polyhalogenated tetraarylporphyrins by selective substitution of para fluorines of *meso*-tetrakis(pentafluorophenyl)porphyrins led us to a series of new supramolecular systems **12a**−**g** illustrated in Figure 1. These include a wide variety of

† Dedicated to Kent R. Wilson.

* To whom correspondence should be addressed. E-mail: cperrin@ucsd.edu. Fax: (858)-822-0386.

‡ University of California—San Diego.

§ Universidade Federal de Pernambuco.

|| Present address: Mesa State College, Grand Junction, CO 81502.

⊥ Present Address: Ecole Normale Superieure, 75231 Paris, France.

▽ Universidade de São Paulo.

⊗ Deceased, June 23, 1993.

10.1021/jp991766s CCC: $18.00
Published on Web 11/09/1999

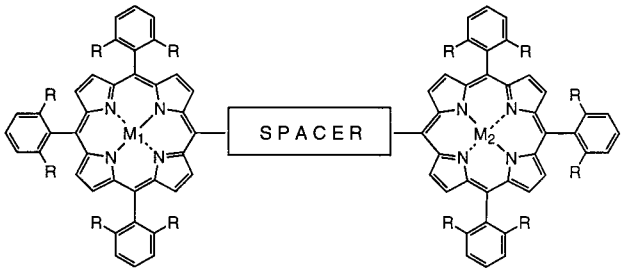

8 $M_1 = M_2 =$ Zn
9 $M_1 = M_2 = H_2$
10 $M_1 = H_2$, M_2 = Zn
11 M_1 = Fe(III)-OAc, $M_2 = H_2$
12 M_1 = Fe(III)-OAc, M_2 = Zn

Compound	Spacer	R
a	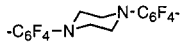	H
b	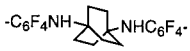	H
c	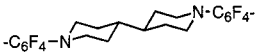	H
d	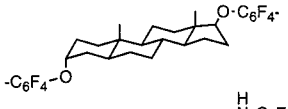	H
e[a]	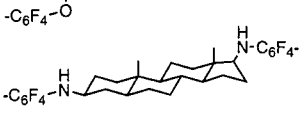	H
f	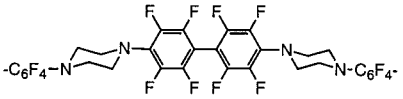	H
g	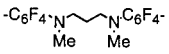	Cl

[a] Mixture of regioisomers for **10-12**

Figure 1. Porphyrin dimers for study of the dependence of ET rate on distance.

spacers, namely, piperazyl (pip), bicyclo[2.2.2]octane-1,4-diamine (bcoda), 4,4′-bipiperidyl (bip), the steroidal diamine 5α-androstanyl-3β,17β-diamine (stda), the steroidal diether 5α-androstanyl-3α,17β-diether (stde), bis(piperazyl)perfluorobiphenylyl (pip-pfbp-pip), and *N*,*N*′-dimethyl-1,3-diaminopropyl (dmdap), each linked to the two porphyrins by a tetrafluorophenyl group. The further tasks are to insert two different metals, so as to allow PET, and to characterize the various porphyrin derivatives, which is not trivial for substances of such high molecular weight. These porphyrin dimers then permit the study of the dependence of electron-transfer rates on distance and on the molecular structure of the intervening linkage. In this series the other critical parameters governing PET rates, such as driving force, reorganization energy, and orientation, can be kept constant. In particular, the electron transfer is always from a singlet excited-state Zn porphyrin to the six-coordinate low-spin Fe(III) complex of the identical porphyrin.

Experimental Section

Materials. All solvents were purchased from Fisher, dried, and distilled by standard methods. All reagents were purchased from Aldrich, Sigma, or Fluka and used as received unless otherwise noted. THF was distilled under argon from sodium benzophenone ketyl immediately prior to use. Pyrrole was distilled from CaH_2 under reduced pressure prior to use. *N*,*N*′-Dimethylpropanediamine (Aldrich) was dried over molecular sieves. Solvents for physical measurements were of spectrophotometric grade.

General Methods. ^{1}H, ^{19}F, and ^{13}C NMR spectra were measured on either a 500-MHz Varian Unity or a 300-MHz GE QE spectrometer, in $CDCl_3$ with tetramethylsilane (TMS) (^{1}H, ^{13}C) or hexafluorobenzene (^{19}F) as the internal standard unless noted otherwise. UV−visible spectra in dichloromethane were recorded on a Kontron Uvikon-810 spectrophotometer. Molar absorption coefficients were determined on 2−3 mg of a compound, weighed accurately, and diluted to an appropriate absorbance. All reactions were carried out under an argon atmosphere in purified solvents with shielding from light and were followed by thin-layer chromatography (silica gel on aluminum foil, Merck 5554). Preparative column chromatography was performed on silica gel (Davisil grade 643 type 150A, 230−435 mesh) or neutral alumina (Brockman Activity I, 60−325 mesh). Mass spectral analyses were conducted by The Scripps Research Institute Mass Spectrometry Facility, La Jolla, CA, by FAB$^+$, EI$^+$, or electrospray$^+$ techniques. These molecules are so large that the peak calculated for the lightest isotopes is not the most prominent, so that sometimes only the most abundant is reported, and this does agree with the calculated peak. Microanalyses were performed by Desert Analytical, Tucson, AZ.

Samples for fluorescence measurements were prepared at concentrations of ca. 1×10^{-5} M in dichloromethane containing 0.01 M 1-methylimidazole. The excitation source was a mode-locked argon ion laser coupled to a synchronously pumped cavity-dumped dye laser operating at 568 nm. Fluorescence decay at 610, 650, or 670 nm was monitored by time-correlated single-photon counting (TCSPC).[21,22] Further details have been described elsewhere.[22]

The fluorescence lifetime of the reference dimer is given by eq 1, where k_F, k_{ISC}, and k_{IC} are the rate constants for

$$\tau_0 = 1/(k_F + k_{ISC} + k_{IC}) \quad (1)$$

fluorescence, intersystem crossing, and nonradiative internal conversion, respectively. If the only additional deactivation pathway available for the Zn,Fe derivatives is the electron transfer and if the rate constants for all of the other deactivation pathways are the same as those in the corresponding reference dimer, the fluorescence lifetimes of the Zn,Fe dimers are given by eq 2. This assumes that energy transfer does not contribute

$$\tau = 1/(k_F + k_{ISC} + k_{IC} + k_{ET}) \quad (2)$$

to the deactivation,[16a,19] an issue that is further addressed below. It then follows that the electron-transfer rate constant k_{ET} can be obtained from the observed fluorescence lifetimes as in eq 3. Experimental values are averaged over data sets from different

$$k_{ET} = 1/\tau - 1/\tau_0 \quad (3)$$

preparations on at least two different days, with at least two measurements at each of two wavelengths on each day.

Distance Measures. It is necessary to establish a measure of the spatial distance between the donor and acceptor in these porphyrin dimers. We have chosen the distance between porphyrin edges. The through-space distance (d_{space}) is the length

of the vector connecting the *meso*-carbons of the zinc and iron porphyrins that are bonded directly to the bridge. The through-bond distance (d_{bond}) is the sum of the lengths of the bonds connecting the *meso*-carbons of the zinc and iron porphyrins that are bonded directly to the bridge. The number of bonds present in the shortest pathway across the bridge connecting the zinc and iron porphyrins at their *meso*-carbon atoms is the total bond pathway (N_{bonds}). The through-space and through-bond distances were calculated by using a Monte Carlo conformation search and MM2 force field. For the more complex stde and stda bridges of **8d**, **12d**, **8e**, and **12e**, d_{space} corresponds to an average over representative conformers selected from a series of low-energy minima.

Even though the linkages may permit rotation of the porphyrins relative to the bridge, and also within the bipiperidyl and bis(piperazyl)perfluorobiphenylyl bridges, those rotations do not greatly change the distance between the two porphyrin edges. This is a consequence of the rigidity of the piperazine, bicyclooctane, and piperidine rings. For the bicyclooctane and steroidal linkages, rotation around the inner C−N or C−O bonds could lead to conformational heterogeneity, if it is slow relative to fluorescence, but the data below show that this complication does not intrude.

An alternative is to choose the metal−metal distance, although this is conformation-dependent and less well-defined. Besides, the donor wave function of ^{1}ZnP* and the acceptor wave function of Fe^{III}P[bis(imidazole)] are both delocalized over their entire porphyrin rings. Therefore, it is reasonable to measure distances in porphyrin dimers simply between porphyrin edges.

Porphyrin Syntheses and Characterization

5-(Pentafluorophenyl)-10,15,20-triphenyl-21*H*,23*H*-porphine (H_2TPPF$_5$, 1). Freshly distilled dichloromethane (2.5 L) in a two-neck, round-bottomed flask protected from light and fitted with septa was stirred and purged with argon for 1 h at room temperature. Then benzaldehyde (5.0 mL, 49 mmol), pentafluorobenzaldehyde (0.86 mL, 7.0 mmol), pyrrole (4.0 mL, 59 mmol), and 2,2-dimethoxypropane (4.0 mL, 33 mmol) were added via syringe in this order. The stirring and bubbling with argon was continued for an additional 15 min, when boron trifluoride etherate (1.6 mL, 13 mmol) was added via syringe in two portions at 30-min intervals. After this addition was completed, the reaction mixture changed immediately from colorless to red-brown. The dark reaction mixture was then stirred for 1.5 h with a slow stream of argon passing through the solution. A solution of 2,3-dichloro-5,6-dicyanobenzoquinone (DDQ; 10.2 g, 45 mmol) in freshly distilled toluene (100 mL) was then added via a cannula needle. The mixture was stirred for an additional 5 h. A longer condensation or oxidation time leads to a larger amount of polymeric material, decreases the overall yield, and causes purification difficulties. The solvent was evaporated to dryness in vacuo. The crude mixture (purple-black powder) was flash chromatographed (neutral alumina: toluene/dichloromethane = 1/3) to remove polar substances. The mixture of products was purified by gradient column chromatography (neutral alumina: petroleum ether/dichloromethane = 6/1 gradually to 3/1) to yield 5,10,-15,20-tetrakis(pentafluorophenyl)-21*H*,23*H*-porphine (0.07 g, 2%) as purple crystals, 5,10,15,20-tetraphenyl-21*H*,23*H*-porphine (0.16 g, 7.4%), and the desired compound **1** (0.71 g, 29%) as purple crystals: ^{1}H NMR δ 8.95−8.75 (m, 8H), 8.25−8.20 (m, 6H), 7.81−7.70 (m, 9H), −2.57 (s, 2H, NH); UV λ_{max} ($10^{-4}\epsilon$) 396 (sh) (8.61), 416 (42.3), 513 (1.9), 548 (0.57), 588 (0.58), 643 (0.26) nm. Anal. Calcd for $C_{44}H_{25}N_4F_5$: C, 74.99; H, 3.58; N, 7.95. Found: C, 75.29; H, 3.55; N, 7.97.

5-(Pentafluorophenyl)-10,15,20-triphenylporphinatozinc (ZnTPPF$_5$, 2). A solution of **1** (0.43 g, 0.61 mmol) and zinc acetate dihydrate (0.81 g, 3.68 mmol) in dichloromethane (90 mL) plus methanol (90 mL) was heated to reflux for 5 h under argon in the dark. The reaction mixture was then cooled to room temperature and concentrated approximately three-fold by evaporation of solvent in vacuo. The residue was diluted with dichloromethane (600 mL) and washed with water (3 × 100 mL), saturated sodium bicarbonate solution (3 × 100 mL), and brine (3 × 100 mL). The water layers were combined and rewashed with dichloromethane (2 × 50 mL). The combined organic layer was dried over sodium sulfate, filtered, and evaporated in vacuo to dryness. The crude product was purified by column chromatography (silica gel: petroleum ether/dichloromethane = 4/1) to yield **2** (0.460 g, 97%) as a pinkish-purple solid: ^{1}H NMR δ 9.02 (d, 2H, J = 5 Hz, pyrrole), 8.94 (d, 4H, J = 3.5 Hz, pyrrole), 8.85 (d, 2H, J = 5 Hz, pyrrole), 8.35−8.15 (m, 6H), 7.88−7.70 (m, 9H); ^{19}F NMR δ 24.62 (dd, 2F, J = 24 and 8 Hz, *o*), 8.41 (t, 1F, J = 24 Hz, *p*), −0.76 (dt, 2F, J = 24 and 8 Hz, *m*); UV λ_{max} 416 (s), 547 (w), 585 (w) nm. Anal. Calcd for $C_{44}H_{23}N_4F_5Zn$: C, 68.84; H, 3.02; N, 7.29. Found: C, 69.08; H, 2.86; N, 7.37.

5-(Pentafluorophenyl)-10,15,20-tris(2,6-dichlorophenyl)-21*H*,23*H*-porphyrin (H_2TPPCl$_6$F$_5$, 3).[23] A 3-L three-neck, round-bottomed flask, equipped with a reflux condenser and an argon inlet, was charged with dry dichloromethane (1400 mL), 2,6-dichlorobenzaldehyde (2.45 g, 14.0 mmol), pentafluorobenzaldehyde (0.25 mL, 2.0 mmol), and pyrrole (1.14 mL, 16.0 mmol). The mixture was stirred and purged with argon for >20 min, after which BF_3·Et_2O (40 mL) was added. The solution rapidly turned dark yellow and then orange-red. The mixture was stirred for 12 h at room temperature. Another portion of BF_3·Et_2O (20 mL) was added, and the solution was stirred for 24 h more. Tetrachloro-1,4-benzoquinone (*p*-chloranil; 3.93 g, 20 mmol) was then added to the dark solution. After refluxing for 4 h, the green solution was concentrated in vacuo to about 100 mL. Neutral alumina (10−20 g) was added, and the residual solvent was removed by evaporation in vacuo. This material was first flash chromatographed (neutral alumina: toluene/dichloromethane = 1/1), concentrated, and then purified by gradient column chromatography (neutral alumina: petroleum ether/dichloromethane = 3/1 gradually to 1/1) to yield **3** (314 mg, 17%) as purple crystals after recrystallization from dichloromethane/methanol: ^{1}H NMR δ 8.77 (m, 4H, pyrrole), 8.70 (m, 4H, pyrrole), 7.83−7.79 (m, 6H, *m*), 7.74−7.68 (m, 3H, *p*), −2.61(s, 2H, NH); ^{19}F NMR δ 25.40 (dd, 2F, J = 24 and 8 Hz, *o*), 9.25 (t, 1F, J = 24 Hz, *p*), −0.44 (dt, 2F, J = 24 and 8 Hz, *m*); UV λ_{max} ($10^{-4}\epsilon$) 416 (25.6), 512 (1.63), 540 (sh), 587 (0.53), 642 (0.25) nm; MS (CI^+, NH_3) *m*/*z* 911 (M^+, 100%). Anal. Calcd for $C_{44}H_{19}Cl_6F_5N_4$: C, 57.99; H, 2.10; N, 6.15. Found: C, 57.89; H, 2.12; N, 6.05.

5-(Pentafluorophenyl)-10,15,20-tris(2,6-dichlorophenyl)-porphinatozinc (ZnTPPCl$_6$F$_5$, 4). 3 (243 mg, 0.266 mmol) was dissolved in a mixture of dichloromethane (40 mL) and methanol (40 mL). Zinc acetate dihydrate (580 mg, 2.66 mmol) was added, and the reaction mixture was refluxed for 12 h. After cooling to room temperature, the solution was neutralized with a saturated aqueous sodium bicarbonate solution. The organic solvents were evaporated in vacuo. Dichloromethane (200 mL) was added, and the organic layer was washed with water (2 × 50 mL) and brine (2 × 50 mL), dried over sodium sulfate, filtered, and evaporated in vacuo. The residue was recrystallized from dichloromethane/hexane to provide zinc complex **4** (255 mg, 98%) as red-purple crystals: ^{1}H NMR δ 8.85 (m, 4H,

pyrrole), 8.80 (m, 4H, pyrrole), 7.80 (m, 6H, *m*), 7.74−7.68 (m, 3H, *p*); ^{19}F NMR δ 25.15 (dd, 2F, J = 24 and 8 Hz, *o*), 8.67 (t, 1F, J = 24 Hz, *p*), −0.76 (dt, 2F, J = 24 and 8 Hz, *m*); UV λ_{max} ($10^{-4}\epsilon$) 418 (72.4), 510 (sh, 0.35), 548 (2.93), 582 (sh, 0.39) nm; MS (CI^+ NH_3) *m*/*z* 975 (M^+, 100%). Anal. Calcd for $C_{44}H_{17}Cl_6F_5N_4Zn$: C, 54.22; H, 1.76; N, 5.75. Found: C, 54.05; H, 1.97; N, 5.70.

5-(Pentafluorophenyl)-10,15,20-triphenylporphinatoiron-(III) Acetate (FeTPPF$_5$·OAc, 5). A mixture of **1** (100 mg, 0.14 mmol) and ferrous bromide (42 mg, 0.45 mmol) in 10 mL of freshly distilled tetrahydrofuran (THF) was heated to reflux under argon for 2 h. After cooling to room temperature, solvent was evaporated in vacuo and the residue was dissolved in dichloromethane (50 mL), washed with 10% aqueous acetic acid (3 × 15 mL) and brine (3 × 15 mL), and dried over calcium chloride. The solvent was evaporated in vacuo. The residue was crystallized from dichloromethane/hexanes to provide **5** (100 mg, 90%) as a brown-purple solid: UV λ_{max} 375 (sh, w), 415 (s), 509 (w), 580 (w), 648 (w) nm. HRMS *m*/*z* calcd for $C_{46}H_{27}N_4F_5FeO_2$ [$(M + H)^+$]: 818.1404. Found: 818.1401.

5-(Pentafluorophenyl)-10,15,20-tris(2,6-dichlorophenyl)-porphinatoiron(III) Acetate (FeTPPCl$_6$F$_5$·OAc, 6). A mixture of **3** (100 mg, 0.11 mmol) and ferrous bromide (42 mg, 0.45 mmol) in 10 mL of freshly distilled dimethylformamide (DMF) was heated to reflux under argon for 0.5 h. After cooling to room temperature, the mixture was diluted with dichloromethane (50 mL), washed with 10% aqueous acetic acid (3 × 15 mL) and brine (3 × 15 mL), and dried over sodium sulfate. The solvent was evaporated in vacuo, and the remaining DMF was removed by vacuum distillation. The crude mixture was purified by column chromatography (alumina: dichloromethane/methanol = 100/1) to give **6** (91 mg, 81%) as a purple-brown solid: UV λ_{max} ($10^{-4}\epsilon$) 380 (sh, 5.54), 416 (8.92), 511 (1.20), 582 (0.37), 649 (0.33) nm. MS. Calcd for $C_{46}H_{21}N_4F_5FeO_2Cl_6$ [$(M + H)^+$]: 1025. Found: 1025.

ZnTPPF$_4$-pip (7a). A solution of zinc porphyrin **2** (100 mg, 0.13 mmol) and piperazine (112 mg, 1.3 mmol) in freshly distilled dry 1-methyl-2-pyrrolidinone (1.5 mL) was heated to 110−120 °C for 20 h under argon. The reaction mixture was then cooled to room temperature, diluted with dichloromethane (50 mL), and washed with water (3 × 20 mL), a saturated sodium bicarbonate solution (3 × 20 mL), and brine (3 × 20 mL). The water layers were combined and extracted with dichloromethane (2 × 40 mL). The combined organic layer was dried over sodium sulfate, filtered, and evaporated in vacuo. The residual 1-methyl-2-pyrrolidinone was removed by vacuum distillation at 60 °C. Purification by column chromatography (silica gel: dichloromethane/methanol/ammonium hydroxide = 15/1/0.1) provided **7a** (97 mg, 89%) as a purple solid: ^{1}H NMR δ 9.05−8.90 (m, 8H), 8.33−8.10 (m, 6H), 7.90−7.64 (m, 9H), 3.89 (m, 4H), 3.78 (m, 5H); UV λ_{max} 418 (s), 548 (w), 588 (w) nm. MS. Calcd for $C_{48}H_{33}N_6F_4Zn$ [$(M + H)^+$]: 834. Found: 834.

ZnTPPF$_4$-bip (7c). 4,4′-Bipiperidyl was prepared from its commercially available dihydrochloride (362 mg, 1.5 mmol) by treatment with 1 M NaOH (3 mL), to produce a white solid [229 mg, 91%, sublimation > 150 °C, mp 172 °C (lit.[24] 172−173 °C)]: ^{1}H NMR δ 3.02 (d, 4H, J = 11.7 Hz, H2a), 2.50 (dd, 4H, J = 11.4 Hz, H2b), 1.80−1.46 (m, 6H) 1.28−0.95 (m, 6H). A solution of zinc porphyrin **2** (190 mg, 0.248 mmol) and 4,4′-bipiperidyl (125 mg, 0.734 mmol) in freshly distilled dry 1-methyl-2-pyrrolidinone (3 mL) was heated to 110−120 °C for 18 h under argon. The reaction mixture was then cooled to room temperature, diluted with dichloromethane (50 mL), and washed with water (3 × 20 mL), a saturated sodium bicarbonate solution (3 × 20 mL), and brine (3 × 20 mL). The water layers were combined and washed with dichloromethane (2 × 40 mL). The combined organic layer was dried over sodium sulfate, filtered, and evaporated in vacuo, and the residual 1-methyl-2-pyrrolidinone was removed by vacuum distillation at 60 °C. Purification by column chromatography (silica gel: dichloromethane/methanol/ammonium hydroxide = 15/1/0.1) provided **7c** (158 mg, 70%) as a dark purple solid: ^{1}H NMR δ 8.98−8.89 (m, 8H), 8.26−8.23 (m, 6H), 7.76−7.74 (m, 9H), 3.48 (d, 2H, J = 11 Hz), 3.01 (dd, 2H, J = 11 Hz), 1.40−1.28 (m, 1H), 0.99−0.87 (m, 3H), 0.77−0.66 (m, 2H), 0.14−0.11 (bm, 1H), −0.25 to −0.48 (bm, 2H), −0.49 to −0.68 (bm, 1H), −1.02 to −1.44 (bm, 1H), −2.00 to −2.32 (bm, 2H), −2.41 to −2.80 (bm, 1H); ^{13}C NMR δ 150.62, 150.27, 149.99, 143.37, 143.33, 134.63, 134.57, 132.87, 132.03, 131.71, 130.11, 127.38, 126.41, 122.21, 121.15, 51.67 ($2CH_2$), 42.01 ($2CH_2$), 39.56 (CH), 38.25 (CH), 29.22 ($2CH_2$), 25.33 ($2CH_2$); ^{19}F NMR δ 22.48 (bs, 2F), 10.54 (bs, 2F); UV λ_{max} 419 (s), 548 (w), 587 (w) nm. HRMS. Calcd for $C_{54}H_{43}N_6F_4Zn$ [$(M + H)^+$]: 915.2777. Found: 915.2747.

ZnTPPF$_4$-stde (7d) and Zn,Zn(TPPF$_4$)$_2$-stde (8d). Commercially available 5α-androstane-3α,17β-diol (8.8 mg, 0.03 mmol) was added to a mixture of sodium hydride (2.7 mg, 0.07 mmol, 60% dispersion in paraffin) and 1-methyl-2-pyrrolidinone (2 mL) at 5 °C under argon. After 1 h **2** (50 mg, 0.065 mmol) was added, and the reaction mixture was heated to 50 °C for 48 h. After cooling to room temperature, the mixture was poured onto ice water (50 mL) and extracted with dichloromethane (3 × 15 mL). The combined organic layer was dried over sodium sulfate and evaporated to dryness. Purification by column chromatography (silica gel: petroleum ether/dichloromethane = 1/1) gave two compounds, **7d** and **8d**, as purple solids. For the more polar **7d** (6 mg, 19%): ^{1}H NMR δ 9.05−8.90 (m, 8H), 8.25−8.20 (m, 6H), 7.85−7.70 (m, 9H), 4.70−4.60 (m, 1H), 3.30−3.20 (m, 1H), 2.45−2.30 (m, 2H), 2.20−0.52 (m, 26H); UV λ_{max} 418 (s), 548 (w), 584 (w) nm. MS. Calcd for $C_{63}H_{54}N_4F_4O_2Zn$: 2082 (2 × MH^+). Found: 2082 (2 × MH^+). For the less polar **8d** (21 mg, 40%): ^{1}H NMR δ 9.10−8.90 (m, 16H), 8.30−8.20 (m, 12H), 7.85−7.70 (m, 18H), 5.05−4.95 (m, 1H), 4.75−4.60 (m, 1H), 2.60−0.55 (m, 28H); UV λ_{max} 418 (s), 547 (w), 586 (w) nm. MS. Calcd for $C_{107}H_{77}N_8F_8O_2Zn_2$ [$(M + H)^+$]: 1785. Found: 1785.

ZnTPPF$_4$-pip-pfbp (7f). A mixture of **7a** (20.0 mg, 0.024 mmol), perfluorobiphenyl (200 mg, 0.60 mmol), *N*,*N*-diisopropylethylamine (0.2 mL), and dimethyl sulfoxide (DMSO; 0.5 mL) was heated to reflux for 21 h under argon. The volatiles were removed under vacuum. The residue was dissolved in toluene (50 mL) and washed with 5% aqueous acetic acid (25 mL) and brine (25 mL). The organic solution was dried over NaOH pellets, filtered, and evaporated to dryness. The residue was purified by column chromatography (silica gel: petroleum ether/dichloromethane = 1/2). Recrystallization from dichloromethane/hexanes gave **7f** (15 mg, 55%) as a purple solid: ^{1}H NMR δ 9.03 (d, 2H, J = 5 Hz), 8.98−8.93 (m, 6H), 8.25−8.21 (m, 6H), 7.84−7.73 (m, 9H), 3.76 (d, 4H, J = 3.5 Hz), 3.68 (d, 4H, J = 3.0 Hz); ^{19}F NMR δ 24.20−24.10 (m, 2F), 22.27 (dd, 2F, J = 9 and 23 Hz), 21.84−21.66 (m, 2F), 11.586 (dd, 2F, J = 6 and 20 Hz), 10.45 (t, 1F, J = 22 Hz), 10.12 (dd, 2F, J = 9 and 23 Hz), 0.82−0.64 (m, 2F); UV λ_{max} 418 (s), 548 (w), 588 (w) nm. Anal. Calcd for $C_{60}H_{31}F_{13}N_6Zn$: C, 62.76; H, 2.72; N, 7.23. Found: C, 63; H, 2.73; N, 7.14.

ZnTPPCl$_6$F$_4$-dmdap (7g). **4** (130 mg, 0.133 mmol) was dissolved in excess *N*,*N*′-dimethyl-1,3-diaminopropane (1.5 mL)

and stirred for 2 h at 135 °C. After cooling to room temperature, the mixture was diluted with dichloromethane (50 mL), washed with a saturated ammonium chloride solution (2 × 20 mL), water (2 × 20 mL), and brine (2 × 20 mL), dried over magnesium sulfate, filtered, and evaporated in vacuo to dryness. The crude product was recrystallized from chloroform/hexane to yield **7g** (137 mg, 97%) as a purple solid: ^{1}H NMR δ 9.01 (d, 2H, J = 4.5 Hz, pyrrole), 8.75−8.70 (m, 6H, pyrrole), 7.78−7.57 (m, 9H), 3.68 (t, 2H, J = 6.9 Hz), 3.61 (m, 2H), 3.36 (bs, 6H), 3.29 (bs, 1H), 2.38−2.30 (m, 2H); ^{19}F NMR (DMSO-d_6) δ 21.37 (bs, 2F), 11.02 (bs, 2F); UV λ_{max} 419 (s), 550 (w), 589 (w) nm. Anal. Calcd for $C_{49}H_{30}Cl_6F_4N_6Zn$: C, 55.68; H, 2.86; N, 7.95. Found: C, 54.98; H, 2.81; N, 7.86.

ZnTPPF$_4$-bip-CHO (7h). Reaction of ZnTPPF$_5$ **2** with 4,4′-bipiperidyl does not proceed at room temperature in DMF and is extremely slow at 60 °C. Therefore, a solution of **2** (100 mg, 0.13 mmol) and 4,4′-bipiperidyl (225 mg, 1.1 mmol) in freshly distilled dry DMF (8 mL) was heated to 140 °C for 24 h under argon. The reaction mixture was cooled to room temperature, and DMF was removed by vacuum distillation at 40 °C. The residue was redissolved in dichloromethane (150 mL) and washed with water (3 × 30 mL), a saturated sodium bicarbonate solution (3 × 30 mL), and brine (3 × 30 mL). The water layers were combined and rewashed with dichloromethane (2 × 40 mL). The combined organic layer was dried over sodium sulfate, filtered, and evaporated in vacuo to dryness. The crude mixture was purified by column chromatography (silica gel: dichloromethane/methanol = 50/1 and then 25/1) to provide **7h** (0.112 g, 91%) as a dark purple solid: ^{1}H NMR δ 9.01−8.90 (m, 8H), 8.28−8.24 (m, 6H), 7.85−7.72 (m, 9H), 5.29 (s, 1H, CHO), 3.70 (d, 2H, J = 11.4 Hz, H2a), 3.30 (dd, 2H, J = 11.8 Hz, H2b), 3.02 (d, 1H, J = 12.6 Hz), 2.84 (d, 1H, J = 12.9 Hz), 2.49−2.39 (m, 1H), 1.75−1.63 (m, 3H), 1.58−1.40 (m, 3H), 1.39−1.10 (m, 3H), 0.81−0.62 (m, 1H), 0.56−0.35 (m, 1H); ^{13}C NMR δ 159.43 (CHO), 150.55, 150.06, 149.76, 142.95, 134.53, 132.89, 132.19, 131.81, 131.23, 129.94, 127.39, 126.45, 126.39, 52.00 (2 CH_2), 46.04 (CH_2), 40.86 (CH), 40.31 (CH), 39.41 (CH_2), 29.87 (CH_2), 29.71 (CH_2), 29.25 (CH_2), 27.91 (CH_2); ^{19}F NMR δ 22.50 (dd, 2F, J = 9 and 23 Hz), 10.56 (dd, 2F, J = 9 and 23 Hz); UV λ_{max} 419 (s), 547 (w), 586 (w) nm. MS. Calcd for $C_{55}H_{43}F_4N_6OZn$ [$(M + H)^+$]: 943. Found: 943.

Zn,Zn(TPPF$_4$)$_2$-pip (8a). A mixture of **2** (19.7 mg, 25 μmol), **7a** (64 mg, 77 μmol), and tributylamine in dry DMSO (0.25 mL) was heated to 120 °C for 24 h. After cooling to room temperature, the solvent was removed by vacuum distillation at 60−80 °C. The residue was dissolved in dichloromethane (50 mL), washed with a saturated sodium bicarbonate solution (2 × 20 mL) and brine (3 × 20 mL), and dried over sodium sulfate. The solvent was evaporated in vacuo. The residue was purified by column chromatography (silica gel: dichloromethane/petroleum ether = 3/1). The product was recrystallized from dichloromethane/hexanes to yield **8a** (13 mg, 33%) as purple crystals: ^{1}H NMR δ 9.07 (d, 4H, J = 4.5 Hz), 9.02 (d, 4H, J = 4.5 Hz), 8.97 (m, 8H), 8.27−8.22 (m, 12H), 7.85−7.70 (m, 18H), 3.94 (s, 8H); UV λ_{max} 419 (s), 547 (w), 587 (w) nm. MS. Calcd for $C_{92}H_{55}N_{10}F_8Zn_2$ [$(M + H)^+$]: 1579. Found: 1582 (most abundant).

Zn,Zn(TPPF$_4$)$_2$-bcoda (8b). A solution of zinc porphyrin **2** (205 mg, 0.267 mmol), bicyclo[2.2.2]octane-1,4-diamine[25] (15 mg, 0.107 mmol), and tributylamine (0.64 mL, 0.267 mmol) in freshly distilled dry 1-methyl-2-pyrrolidinone (3 mL) was heated to 150−160 °C for 48 h under argon. The reaction mixture was cooled to room temperature, diluted with dichloromethane (50 mL), and washed with water (3 × 10 mL), a saturated sodium bicarbonate (3 × 10 mL), and brine (3 × 10 mL). The water layers were combined and washed with dichloromethane (2 × 40 mL). The combined organic layer was dried over sodium sulfate, filtered, and evaporated in vacuo, and the residual 1-methyl-2-pyrrolidinone was removed by vacuum distillation at 60 °C. Purification by column chromatography (silica gel: dichloromethane/methanol/ammonium hydroxide = 15/1/0.1) provided **8b** (60 mg, 34%) as a dark purple solid: ^{1}H NMR δ 9.06−8.92 (m, 16H), 8.28−8.20 (m, 12H), 7.84−7.70 (m, 18H), 2.26 (s, 12H); UV λ_{max} 419 (s), 547 (w), 585 (w) nm. MS. Calcd for $C_{96}H_{61}N_{10}F_8Zn_2$ [$(M + H)^+$]: 1633. Found: 1633.

Zn,Zn(TPPF$_4$)$_2$-bip (8c). A solution of zinc porphyrin **7c** (65.6 mg, 0.071 mmol), **2** (100 mg, 0.14 mmol), and tributylamine (0.034 mL, 0.14 mmol) in freshly distilled dry 1-methyl-2-pyrrolidinone (1 mL) was heated to 110−120 °C for 24 h under argon. After cooling to room temperature, the mixture was diluted with dichloromethane (50 mL) and washed with water (3 × 20 mL), a saturated sodium bicarbonate solution (3 × 20 mL), and brine (3 × 20 mL). The water layers were combined and rewashed with dichloromethane (2 × 40 mL). The combined organic layer was dried over sodium sulfate. The solvent was evaporated in vacuo, and the residual 1-methyl-2-pyrrolidinone was removed by vacuum distillation at 60 °C. Purification by column chromatography (silica gel: dichloromethane/methanol = 50/1) gave **8c** (78 mg, 66%) as a purple solid: ^{1}H NMR δ 9.10−8.90 (m, 8H), 8.25−8.21 (m, 6H), 7.78−7.73 (m, 9H), 3.88−3.83 (m, 2H), 3.51−3.46 (m, 2H), 2.18−2.12 (m, 2H), 2.10−2.02 (m, 2H), 1.81−1.71 (m, 2H), 1.64−1.53 (m, 2H), 1.29−1.23 (m, 2H), 1.03−0.90 (m, 2H), 0.90−0.83 (m, 2H); UV λ_{max} 419 (s), 547 (w), 585 (w) nm. MS. Calcd for $C_{98}H_{65}N_{10}F_8Zn_2$ [$(M + H)^+$]: 1661. Found: 1663, 1665 (most abundant).

Zn,Zn(TPPF$_4$)$_2$-stda (8e). 5α-Androstane-3β,17β-diamine was prepared by oxidation of epiandrosterone followed by reductive amination.[26] A solution of this amine (5.2 mg, 0.018 mmol), **2** (30 mg, 0.039 mmol), and tributylamine (0.013 mL, 0.053 mmol) in freshly distilled dry 1-methyl-2-pyrrolidinone (1 mL) was heated to 140−150 °C for 72 h under argon. The reaction mixture was worked up in the usual manner. Purification by column chromatography (silica gel: dichloromethane/petroleum ether = 1/1) gave **8e** (7.5 mg, 23%) as a purple solid: ^{1}H NMR δ 9.30−8.88 (m, 16H), 8.25−8.19 (m, 12H), 7.82−7.72 (m, 18H), 4.65−4.54 (m, 1H), 4.00−3.94 (m, 1H), 2.50−0.50 (m, 28H); UV λ_{max} 418 (s), 548 (w), 586 (w) nm. MS. Calcd for $C_{107}H_{79}N_{10}F_8Zn_2$ [$(M + H)^+$]: 1783. Found: 1783.

Zn,Zn(TPPF$_4$)$_2$-pip-pfbp-pip (8f). A mixture of **7f** (10 mg, 0.0087 mmol), **7a** (15 mg, 0.018 mmol), 1-ethyl-2,2,6,6-tetramethylpiperidine (0.1 mL), and dry DMSO (0.5 mL) was heated to 120 °C for 44 h under argon. The mixture was cooled to room temperature, diluted with toluene (50 mL), and washed with 5% aqueous acetic acid (2 × 25 mL), saturated sodium bicarbonate (2 × 25 mL), and brine (2 × 20 mL). The organic solution was dried over sodium sulfate, filtered, and evaporated to dryness. The residue was purified by column chromatography (silica gel: petroleum ether/dichloromethane = 1/1). Recrystallization from dichloromethane/hexanes gave **8f** (10 mg, 59%) as a purple solid: ^{1}H NMR δ 9.03 (d, 4H, J = 5.0 Hz), 8.98−8.94 (m, 12H), 8.26−8.20 (m, 12H), 7.82−7.73 (m, 18H), 3.82 (d, 8H, J = 3.5 Hz), 3.68 (d, 8H, J = 3.0 Hz); ^{19}F NMR δ 22.20 (dd, 4F, J = 9 and 23 Hz), 21.64 (dd, 4F, J = 5, 19 Hz), 11.21 (bd, 4F, J = 15 Hz), 10.11 (dd, 4F, J = 9, 23 Hz); UV

λ_{max} 417 (s), 549 (w), 586 (w) nm. Anal. Calcd for $C_{108}H_{62}F_{16}N_{12}Zn_2$: C, 66.10; H, 3.18; N, 8.56. Found: C, 65.91; H, 3.36; N, 7.96.

Zn,Zn(TPPCl$_6$F$_4$)$_2$-dmdap (8g). Amine **7g** (62.0 mg, 0.059 mmol), **4** (28.6 mg, 0.029 mmol), and tributylamine (6.9 μL, 0.029 mol) were dissolved in dry DMSO (300 μL) under an argon atmosphere and stirred at 130 °C for 10 h. After cooling to room temperature, the solution was diluted with dichloromethane (100 mL). The organic phase was washed with a saturated ammonium chloride solution (3 × 10 mL) and brine (3 × 10 mL). After drying over magnesium sulfate, the solvent was evaporated in vacuo. The crude mixture was purified by column chromatography (silica gel: petroleum ether/dichloromethane = 3:1) to give **8g** (32 mg, 54% based on **4**) as a purple solid: ^{1}H NMR δ 8.96 (d, 4H, J = 4.5 Hz, pyrrole), 8.74 (d, 4H, J = 4.5 Hz, pyrrole), 8.73(d, 4H, J = 4.5 Hz, pyrrole), 8.70 (d, 4H, J = 4.5 Hz, pyrrole), 7.76 (d, 4H, J = 8 Hz, *m*), 7.71−7.66 (m, 10H, J = 8 Hz, phenyl), 7.57 (t, 4H, J = 8 Hz, *p*), 3.71 (t, 4H, J = 6.8 Hz, N−CH$_2$), 3.34 (s, 6H, CH$_3$), 2.31 (qn, 2H, J = 6.8 Hz, CH$_2$); ^{19}F NMR δ 22.27 (d, 4F, J = 16 Hz), 10.50 (d, 4F, J = 16 Hz); UV λ_{max} ($10^{-4}\epsilon$) 419 (26), 549 (1.6), 585 (sh) nm. MS (FAB+, CH_2Cl_2/NBA). Calcd for $C_{93}H_{47}Cl_{12}F_8N_{10}Zn_2$ [(M + H)$^+$]: 2003. Found: 2012 (most abundant).

H$_2$,H$_2$(TPPF$_4$)$_2$-pip (9a). A solution of **8a** (15 mg, 9.5 mmol) in dichloromethane (15 mL) was vigorously stirred with 25% aqueous hydrochloric acid (10 mL) for 20 h. The organic layer was separated, diluted with dichloromethane (50 mL), washed with water (3 × 15 mL), 10% NaOH (2 × 15 mL), and brine (3 × 15 mL), and dried over NaOH pellets. The solution was decanted, the solvent was evaporated, and the residue was recrystallized from dichloromethane/hexanes to yield **9a** (13 mg, 87%) as purple crystals: ^{1}H NMR δ 8.96 (d, J = 4.5 Hz, 4H), 8.92 (d, J = 4.5 Hz, 4H), 8.93−8.31 (m, 8H), 8.27−8.22 (m, 12H), 7.84−7.74 (m, 18H), 3.93 (s, 8H), −2.73 (s, 4H); UV λ_{max} 418 (s), 513 (w), 548 (w), 588 (w), 643 (w) nm. Anal. Calcd for $C_{92}H_{58}F_8N_{10}$: C, 75.92; H, 4.02; N, 9.62. Found: C, 76.19; H, 3.99; N, 9.39.

H$_2$,H$_2$(TPPF$_4$)$_2$-bcoda (9b). A mixture of **8b** (20 mg, 12.2 mmol), dichloromethane (20 mL), methanol (2 mL), and aqueous hydrochloric acid (1M, 10 mL) was stirred for 10 h at room temperature. The reaction mixture was worked up according to the procedure for **9a**. After evaporation of the solvent, the residue was taken up in CH_2Cl_2 and precipitated with pentane to yield **9b** (15 mg, 83%) as a dark purple solid: ^{1}H NMR δ 8.98−8.92 (m, 16H), 8.18−8.28 (m, 12H), 7.82−7.72 (m, 18H), 2.30 (s, 12H), −2.75 (s, 4H); UV λ_{max} 418 (s), 514 (w), 549 (w), 591 (w), 644 (w) nm.

H$_2$,H$_2$(TPPF$_4$)$_2$-stda (9e). A mixture of **8e** (4 mg, 0.002 mmol) in dichloromethane (5 mL) and methanol (0.5 mL) was treated with aqueous hydrochloric acid (1 M, 1 mL) for 12 h, followed by the usual workup. After evaporation of the solvent, the residue was taken up in CH_2Cl_2 and precipitated with pentane to yield **9e** (3 mg, 91%) as a dark purple solid: ^{1}H NMR δ 9.27−8.82 (m, 16H), 8.28−8.15 (m, 12H), 7.80−7.70 (m, 18H), 4.50−4.40 (m, 1H), 3.90−3.70 (m, 1H), 2.50−0.50 (m, 28H), −2.70 (s, 4H); UV λ_{max} 417 (s), 513 (w), 548 (w), 589 (w), 643 (w) nm.

H$_2$,H$_2$(TPPF$_4$)$_2$-pip-pfbp-pip (9f). A solution of **8f** (50 mg, 0.025 mmol) in dichloromethane (25 mL) was vigorously stirred with 25% aqueous HCl (20 mL) for 20 h. The organic layer was separated, diluted with dichloromethane (50 mL), washed with water (3 × 20 mL), 10% NaOH (2 × 20 mL), and brine (3 × 20 mL), and dried over NaOH pellets. The solution was decanted, the solvent was evaporated, and the residue was recrystallized from methylene chloride/hexanes to yield **9f** (40 mg, 88%) as purple crystals. ^{1}H NMR δ 9.00 (d, 4H, J = 5.1 Hz), 8.98−8.91 (m, 12H), 8.27−8.18 (m, 12H), 7.84−7.74 (m, 18H), 3.80 (d, 8H, J = 3.5 Hz), 3.69 (d, 8H, J = 3.1 Hz), −2.73 (s, 4H); UV λ_{max} 418 (s), 513 (w), 547 (w), 587 (w), 643 (w) nm. Anal. Calcd for $C_{108}H_{66}F_{16}N_{12}$: C, 70.66; H, 3.62; N, 9.16. Found: C, 70.79; H, 3.55; N, 8.97.

H$_2$,H$_2$(TPPCl$_6$F$_4$)-dmdap (9g). Dimer **8g** (21 mg, 0.0104 mmol) was dissolved in dichloromethane (30 mL) and mixed with 25% aqueous hydrochloric acid (5 mL). After 12 h of reflux, a brownish green solution was obtained. Two phases were separated. The dichloromethane layer was washed with water until the pH was neutral, whereupon the organic layer changed to dark red. The solution was then dried over sodium sulfate, concentrated by evaporation in vacuo, and purified by column chromatography (silica gel: petroleum ether/dichloromethane = 1/1) to obtain **9g** (16 mg, 80%) as a purple solid: ^{1}H NMR δ 8.90 (d, 4H, J = 4.5 Hz, pyrrole), 8.69 (d, 4H, J = 4.5 Hz, pyrrole), 8.68 (d, 4H, J = 4.5 Hz, pyrrole), 8.65 (d, 4H, J = 4.5 Hz, pyrrole), 7.79 (d, 4H, J = 8 Hz, *m*), 7.69 (t, 2H, J = 8 Hz, *p*), 7.67 (m, 8H, J = 8 Hz, *m*), 7.53 (t, 4H, J = 8 Hz, *p*), 3.71 (t, 4H, J = 7.5 Hz, N−CH$_2$), 3.35 (s, 6H, CH$_3$), 2.33 (qn, 2H, J = 7.5 Hz, CH$_2$), −2.60 (s, 4H, NH); ^{19}F NMR δ 22.47 (dd, 4F, J = 23 and 8 Hz), 10.63 (dd, 4F, J = 23 and 8 Hz); UV λ_{max} ($10^{-4}\epsilon$) 418 (61), 512 (4.2), 543 (0.6), 588 (1.3), 645 (0.1) nm. Anal. Calcd for $C_{93}H_{50}Cl_{12}F_8N_{10}$: C, 59.26; H, 2.67; N, 7.73. Found: C, 59.08; H, 2.69; N, 7.59.

Zn,H$_2$(TPPF$_4$)$_2$bip (10c). A solution of zinc porphyrin **7c** (65.6 mg, 0.071 mmol), **1** (100 mg, 0.14 mmol), and tributylamine (0.034 mL, 0.14 mmol) in freshly distilled dry 1-methyl-2-pyrrolidinone (1 mL) was heated to 110−120 °C for 24 h under argon. The reaction mixture was cooled to room temperature, diluted with dichloromethane (50 mL), and washed with water (3 × 20 mL), a saturated sodium bicarbonate solution (3 × 20 mL), and brine (3 × 20 mL). The water layers were combined and rewashed with dichloromethane (2 × 40 mL). The combined organic layer was dried over sodium sulfate, filtered, and evaporated in vacuo, and the residual 1-methyl-2-pyrrolidinone was removed by vacuum distillation at 60 °C. Purification by column chromatography (silica gel: dichloromethane/methanol = 50/1) gave **10c** (78 mg, 66%) as a purple solid: ^{1}H NMR δ 9.05−8.49 (m, 16H), 8.26−8.21 (m, 12H), 7.82−7.75 (m, 18H), 3.90−3.85 (m, 2H), 3.52−3.42 (m, 2H), 2.10−2.02 (m, 2H), 1.77−1.72 (m, 2H), 1.62−1.55 (m, 1H), 1.55−1.44 (m, 3H), 1.32−1.21 (m, 3H), 0.93−0.75 (m, 3H), −2.69 (s, 2H); UV λ_{max} 419 (s), 510 (w), 548 (w), 585 (w), 622(w) nm. HRMS. Calcd for $C_{98}H_{67}N_{10}F_8Zn$ [(M + H)$^+$]: 1599.47. Found: 1599.6.

Zn,H$_2$(TPPF$_4$)$_2$stde (10d). Solid **7d** (3 mg, 2.8 μmol) was added to a mixture of sodium hydride (0.53 mg, 0.013 mmol, 60% dispersion in paraffin) and 1-methyl-2-pyrrolidinone (1 mL) at 5 °C under argon. After 1 h **1** (10 mg, 0.014 mmol) was added, and the mixture was heated to 50 °C for 48 h. After cooling to room temperature, the mixture was poured onto ice water (50 mL) and washed with dichloromethane (3 × 15 mL). The combined organic layer was dried over sodium sulfate and evaporated to dryness. Purification by column chromatography (silica gel: petroleum ether/dichloromethane = 1/1) gave **10d** (1.9 mg, 38%) as a purple solid: ^{1}H NMR δ 9.10−8.80 (m, 16H), 8.20−8.10 (m, 12H), 7.80−7.70 (m, 18H), 5.00−4.90 (m, 1H), 4.90−4.80 (m, 1H), 2.60−0.50 (m, 28H), −2.70 (s, 2H); UV λ_{max} 419 (s), 510 (w), 548 (w), 585 (w), 620(w) nm.

Zn,Fe(TPPF$_4$)$_2$-pip·OAc (12a). A mixture of dimer **9a** (8.5 mg, 5.8 μmol) and ferrous bromide (1.25 mg, 5.8 μmol) in freshly distilled THF (15 mL) was heated to reflux for 1.5 h under argon. At this time additional ferrous bromide (1.0 mg, 4.6 μmol) was added and heating was continued for 24 h. After cooling to room temperature, the reaction mixture was exposed to air for 30 min to allow the spontaneous oxidation of iron(II) to iron(III), and the solvent was evaporated in vacuo. The residue was dissolved in dichloromethane (30 mL), washed with a 10% NaOH solution (2 × 10 mL), and dried over NaOH pellets. The solution was decanted, and the solvent was evaporated in vacuo. The crude mixture was purified by column chromatography (silica gel: dichloromethane/methanol = 100/1) to give monometalated dimer **11a** (8.3 mg, 60%) as a purple-brown solid. Without further characterization monometalated dimer **11a** was dissolved in a dichloromethane/methanol = 2/1 solution (10 mL). Zinc acetate dihydrate (100 mg, 0.045 mmol) was added, and the mixture was heated to reflux for 2 h. After cooling to room temperature, the solvent was evaporated in vacuo. The residue was dissolved in dichloromethane (25 mL), washed with water (2 × 15 mL) and 5% aqueous acetic acid (3 × 15 mL), and dried over sodium sulfate. After evaporation of the solvent, the residue was purified by column chromatography (silica gel: 1% methanol in dichloromethane) to yield the single species **12a** (5.5 mg, 58%): UV λ_{max} 418 (s), 509 (w), 547 (w) nm. MS. Calcd for $C_{94}H_{60}N_{10}F_8O_2FeZn$ [$(M + H)^+$]: 1632. Found: 1632.

Zn,Fe(TPPF$_4$)$_2$-bcoda·OAc (12b). A mixture of dimer **9b** (4.5 mg, 3.0 μmol) and ferrous bromide (0.65 mg, 3.0 μmol) in freshly distilled THF (1 mL) was heated to reflux for 24 h under argon. After the usual workup, the crude mixture was purified by column chromatography (silica gel: dichloromethane/methanol = 50/1) to give monometalated dimer **11b** (3 mg, 64%) as a purple-brown solid. Without further characterization, monometalated dimer **11b** and zinc acetate dihydrate (50 mg, 0.02 mmol) were heated to reflux in dichloromethane/methanol = 1/1 (5 mL) for 2 h. After cooling to room temperature, the solvent was evaporated in vacuo. The residue was dissolved in dichloromethane (25 mL), washed with water (2 × 15 mL) and 5% aqueous acetic acid (3 × 15 mL), and dried over sodium sulfate. After evaporation of the solvent, the residue was purified by column chromatography (silica gel: 1% methanol in dichloromethane) to yield **12b** (2 mg, 65%): UV λ_{max} 418 (s), 512 (w), 547 (w) nm. MS. Calcd for $C_{98}H_{64}N_{10}F_8O_2FeZn$ [$(M + H)^+$]: 1684. Found: 1684.

Zn,Fe(TPPF$_4$)$_2$-bip·OAc (12c). A mixture of dimer **10c** (66 mg, 0.041 mmol) and ferrous bromide (17.4 mg, 0.078 mmol) in freshly distilled dry THF (5 mL) was heated to reflux for 2 h under argon. After cooling to room temperature, the reaction mixture was aerated for 30 min. The reaction mixture was then diluted with dichloromethane (60 mL) and washed with 5% aqueous acetic acid (3 × 20 mL) and water (3 × 20 mL). The water layers were combined and rewashed with dichloromethane (2 × 20 mL). The combined organic layer was dried over sodium sulfate, filtered, and evaporated in vacuo to dryness. The crude mixture was purified by column chromatography (silica gel: dichloromethane/methanol = 50/1) to yield **12b** (0.064 g, 88%): UV λ_{max} 418 (s), 513 (w), 548 (w) nm. MS. Calcd for $C_{100}H_{69}N_{10}F_8O_2FeZn$ [$(M + H)^+$]: 1713. Found: 1713.

Zn,Fe(TPPF$_4$)$_2$-stde·OAc (12d). A mixture of dimer **10d** (2.5 mg, 1.5 μmol) and ferrous bromide (1.56 mg, 7.3 μmol) in freshly distilled dry THF (2 mL) was heated to reflux for 12 h under argon. After the usual workup, the crude mixture was purified by column chromatography (silica gel: dichloromethane/methanol = 50/1) to yield **12d** (1.9 mg, 70%): UV λ_{max} 418 (s), 511 (w), 548 (w) nm. MS. Calcd for $C_{109}H_{81}N_8F_8O_4FeZn$ [$(M + H)^+$]: 1837. Found: 1777 [$(M\text{-}OAc)^+$].

Zn,Fe(TPPF$_4$)$_2$-stda·OAc (12e). A mixture of dimer **9e** (2.2 mg, 1.3 μmol) and ferrous bromide (1.4 mg, 6.6 μmol) in freshly distilled dry THF (1 mL) was heated to reflux for 10 h under argon. After workup and zinc acetate treatment, as for **12b**, the crude mixture was purified by column chromatography (silica gel: dichloromethane/methanol = 50/1) to yield **12e** (1.5 mg, 65%, mixture of regioisomers): UV λ_{max} 418 (s), 513 (w), 547 (w) nm. MS. Calcd for $C_{109}H_{82}N_{10}F_8O_2FeZn$ [$(M + H)^+$]: 1834. Found: 1775 ($M + H^+ - OAc$).

Zn,Fe(TPPF$_4$)$_2$-pip-pfbp-pip·OAc (12f). A mixture of dimer **9f** (10 mg, 0.005 mmol) and ferrous bromide (1.25 mg, 5.8 μmol) in freshly distilled THF (15 mL) was heated to reflux under argon for 10 h. After the usual workup, the crude mixture was purified by column chromatography (silica gel: dichloromethane/methanol = 2/1) to give monometalated dimer **11f** (5.7 mg, 59%) as a purple-brown solid. Without further characterization, monometalated dimer **11c** was dissolved in 10 mL of 1/1 dichloromethane/methanol. Zinc acetate dihydrate (100 mg, 0.045 mmol) was added, and the mixture was stirred at 25 °C for 1.5 h. The reaction was briefly heated to reflux (5−10 min), and the solvent was evaporated in vacuo. The residue was dissolved in dichloromethane (25 mL), washed with water (2 × 15 mL) and 5% aqueous acetic acid (3 × 15 mL), and dried over sodium sulfate. After evaporation of solvent, the residue was purified by column chromatography (silica gel: 1% methanol in dichloromethane) to yield **12f** (5.5 mg, 58%): UV λ_{max} 418 (s), 510 (w), 547 (w) nm. MS. Calcd for $C_{110}H_{66}N_{12}F_{16}O_2FeZn$ [$(M + H)^+$]: 2010. Found: 2012 (most abundant).

Zn,Fe(TPPCl$_6$F$_4$)$_2$-dmdap·OAc (12g). A mixture of dimer **9g** (14.5 mg, 7.7 μmol) and ferrous bromide (1.8 mg, 8.4 μmol) in freshly distilled DMF (2.5 mL) was heated to reflux under argon for 20 min. After this time, additional ferrous bromide (0.5 mg, 2.3 μmol) was added and reflux was continued for 10 min. The reaction mixture was diluted with dichloromethane (50 mL) and washed with water (3 × 20 mL). The solvent was evaporated in vacuo. The crude mixture was purified by column chromatography (alumina: dichloromethane/methanol = 1/1) to give monometalated dimer **11g** (8.3 mg, 63%) as a purple-brown solid. Without further characterization, this was dissolved in 1/1 dichloromethane/methanol (10 mL). Zinc acetate dihydrate (172.2 mg, 0.077 mmol) was added, and the mixture was heated to reflux for 2 h. After cooling to room temperature, the solvent was evaporated in vacuo and the residue was dissolved in dichloromethane (50 mL), washed with 5% aqueous acetic acid (3 × 20 mL) and water (3 × 20 mL), and dried over sodium sulfate. The crude mixture was purified by gradient column chromatography (alumina: dichloromethane, gradually to dichloromethane/methanol = 50/1) to give dimer **12g** (5.5 mg, 63%) as a dark purple solid: UV λ_{max} 417 (s), 510 (w), 549 (w) nm. MS. Calcd for $C_{95}H_{52}Cl_{12}F_8N_{10}O_2FeZn$ [$(M + H)^+$]: 2055. Found: 2061 (most abundant).

Results and Discussion

Considerations of Synthesis. A large part of the effort in the studies of covalently linked donor−acceptor systems lies in the skillful synthesis of tailor-made supramolecular structures.[8,10,13] Dimeric and oligomeric porphyrin arrays have been prepared by several different building-block approaches.[10,16,18−20,27−30]

SCHEME 1[a]

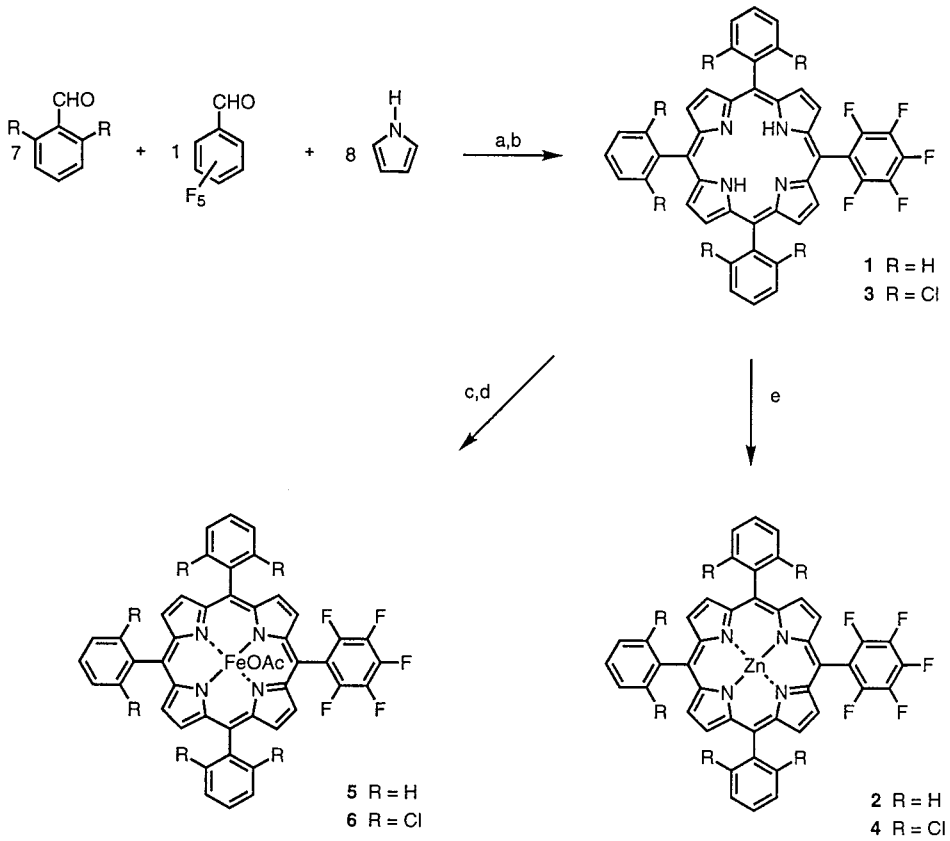

[a] (a) $BF_3{\cdot}OEt_2$, 2,2-dimethoxypropane, CH_2Cl_2, rt, 2 h. (b) DDQ, rt, 5 h, 20−30%. (c) $FeBr_2$, DMF or THF, Δ. (d) Aqueous AcOH. (e) $Zn(OAc)_2{\cdot}2H_2O$, CH_2Cl_2/MeOH, Δ, 98%.

Our synthetic strategy represents an application of a regioselective nucleophilic aromatic substitution previously described in porphyrin chemistry.[20] The regioselectivity of the coupling depends on a porphyrin bearing a single *meso*-pentafluorophenyl group, where only the fluorine at the para position can be successfully substituted with a nitrogen nucleophile. This synthetic methodology allows the systematic modification of many variables in the diporphyrin system, including type and length of spacer, metal center, and redox-potential difference between the donor and acceptor metalloporphyrin. We prepared a set of building blocks suitable for the sequential synthesis of all of the porphyrin dimers in Figure 1.

The reaction scheme calls for a suitable porphyrin with a single *meso*-pentafluorophenyl group (Scheme 1). Stable, crystalline H_2TPPF_5 (**1**) fulfills the basic demands. Its synthesis was accomplished by a modification of the procedure of Lindsey.[31,32] A 7/1 mixture of benzaldehyde and pentafluorobenzaldehyde was condensed with 1 equiv of pyrrole under Lewis acid catalysis ($BF_3{\cdot}Et_2O$) and 2,2-dimethoxypropane as a water scavenger, to provide a presumed porphyrinogen intermediate that was not isolated. Oxidative aromatization with DDQ then provided the desired porphyrin in respectable yield.

Pentafluoroporphyrin **1** is readily metalated with excess zinc acetate to form zinc(II) porphyrin **2**. Because this is stable under basic conditions, it proved to be suitable for nucleophilic substitution with amines. To demonstrate the generality of this method, 2,6-dichlorobenzaldehyde and pentafluorobenzaldehyde were also coupled to form tris(2,6-dichlorophenyl)pentafluoroporphyrin **3**. Metalation of **3** provided zinc porphyrin **4** in excellent yield. The iron(III) porphyrins $FeTPPF_5{\cdot}OAc$ (**5**) and $FeTPPCl_6F_5{\cdot}OAc$ (**6**) could also be prepared by a standard iron insertion method.[33,34]

Heating **2** with excess piperazine in either DMF or 1-methyl-2-pyrrolidinone leads to clean substitution of the para fluorine and conversion to amino derivative **7a** (Scheme 2). This amine was next heated in DMSO with an excess of **2** and tributylamine as a proton scavenger to afford Zn,Zn dimer **8a** in good yield. This two-step procedure, using an excess of one reagent and then the other, was found to be preferable to a single reaction under 2/1 stoichiometry. Hydrolysis of the Zn,Zn dimer **8a** with HCl in methanol/dichloromethane, followed by neutralization, provided free base dimer **9a**. Iron insertion into **9a** was achieved with 1.1 equiv of $FeBr_2$ in refluxing THF, followed by a standard ligand exchange and air oxidation, to provide monometalated iron(III) acetate dimer **11a**. Dimer **11a** underwent zinc insertion to form the donor−acceptor dimer **12a** in 30% yield from **8a**.

The Zn,Zn dimer **8b** was obtained in only 34% yield by a one-step double coupling of **2** with bicyclo[2.2.2]octane-1,4-diamine[25a] and tributylamine in 1-methyl-2-pyrrolidinone. Acid hydrolysis provided **9b**, which was converted to **12b** by sequential treatment with ferrous bromide and zinc acetate.

A different result was obtained when this coupling was attempted toward **8c**. Heating **2** with 4,4′-bipiperidyl in DMF proceeds with clean substitution of the aromatic fluoride. However, subsequent attack of the remaining amine functionality on DMF results in transamidation and formation of formamide **7h** as the sole product. This amide was found to be stable to various reaction conditions and unreactive in additional coupling reactions. When DMF was replaced with 1-methyl-2-pyrrolidinone, which is less prone to transamidation, the reaction of **2** with excess 4,4′-bipiperidyl gave exclusively **7c**. This material showed interesting NMR behavior. The aliphatic CH signals of the 4,4′-bipiperidyl fragment are broad and show an extreme upfield shift, to δ −2.8 ppm in $CDCl_3$. Such broadening was

SCHEME 2[a]

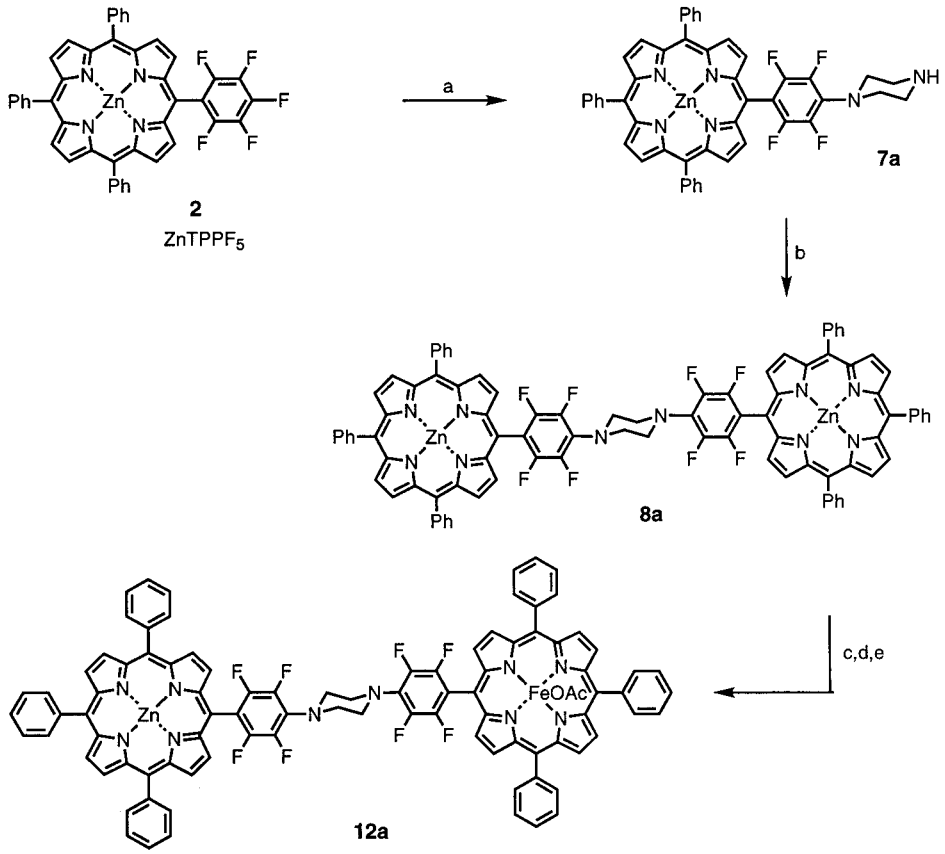

[a] (a) Excess piperazine, 1-methyl-2-pyrrolidinone, 120 °C, 24 h, 96−98%. (b) $ZnTPPF_5$, tributylamine, 1-methyl-2-pyrrolidinone, 130 °C, 24 h, 87%. (c) 1 M HCl in $MeOH/CH_2Cl_2$. (d) $FeBr_2$, THF, Δ. (e) $Zn(OAc)_2 \cdot 2H_2O$, $CH_2Cl_2/MeOH$, Δ, 92%.

not observed in formamide **7h**. At 50 °C some of the multiplets of **7c** sharpen, suggesting a dynamic complexation and decomplexation on the NMR time scale. We propose that the free amino group is cooordinated to the zinc of another molecule, producing a "head to tail" dimer, where the aliphatic protons are shielded by the electron cloud of the second porphyrin. The Zn,Zn dimer **8c** was then obtained by coupling amine **7c** with excess **2**. Alternatively, **7c** could be coupled with an excess of **1** to yield monozinc dimer **10c**. Iron insertion into the free-base porphyrin unit of **10c** was effected with ferrous bromide, followed by acetic acid wash and spontaneous oxidation of Fe(II), leading to the formation of Zn(II),Fe(III) acetate bipiperidyl dimer **12c** in good overall yield.

5α-Androstane-3α,17β-diol was deprotonated with NaH and coupled with **2** to form a mixture of Zn-stde monoporphyrin **7d** (19%) and Zn,Zn dimer **8d** (40%). By comparison of ^{1}H NMR spectra, the structure of **7d** is consistent with a free 3α-hydroxy derivative, which agrees with the greater reactivity of 17β-diol toward esterification.[35] The alcohol **7d** was then added to excess NaH in 1-methyl-2-pyrrolidinone and heated with **1** to produce Zn,H_2 dimer **10d**. Reaction of **10d** with ferrous bromide led to Zn(II),Fe(III) dimer **12d**. Regardless of the assignments for **7d**, **10d**, and **12d**, the distance between the two porphyrins is independent of the regiochemistry.

The Zn,Zn-stda dimer **8e** was obtained by heating 5α-androstane-3β,17β-diamine[26] with 2 equiv of **2**. The mixture of regioisomeric Zn,Fe-stda dimers **12e** could then be obtained by acid hydrolysis to **9e** followed by two successive metal insertions. Again the distance between the two porphyrins is the same for both regioisomers.

The Zn,Fe-piperazyl-octafluorobiphenyl-piperazyl dimer **12f** was made analogously to Scheme 2. Heating amine **7a** with excess perfluorobiphenyl gave **7f**, which after a second coupling with a slight excess of **7a** provided Zn,Zn dimer **8f**. This dimer underwent acid-catalyzed zinc hydrolysis, iron insertion, and a series of ligand-exchange steps to produce **12f**.

Zinc porphyrin **4** was reacted with excess *N*,*N*′-dimethyl-1,3-diaminopropane to form amine **7g**. When **7g** was coupled with half an equivalent of **4**, the Zn,Zn dimer **8g** was obtained. This dimer could be converted in good overall yield to the Zn(II),-Fe(III) dimer **12g** by acid removal of the zinc to produce **9g**, followed by iron insertion, spontaneous oxidation, zinc insertion, and ligand exchange.

Kinetics of PET. Fluorescence lifetimes were measured for the series of metalloporphyrin heterodimers **12a**−**g** as well as for some of their reference homodimers **8a**−**g**. Figure 2 shows representative fluorescence decay curves. Excited-state lifetimes determined from these measurements are presented in Table 1.

The fluorescence decays for nearly all of the porphyrin dimers are monoexponential or else biexponential with a slower component of very low amplitude. A few of the Zn,Fe dimers are exceptions. The Zn,Fe dimer **12a** linked by piperazine (Table 1, entry 5) exhibits triexponential kinetics with one dominant component. Two minor components with slower decays were present, attributable to trace impurities. The lifetime of the third component is similar to that of the Zn,Zn dimer, suggesting the presence of ca. 2% of this compound as well. The Zn,Fe porphyrin dimers **12c** and **12f** (Table 1, entries 9 and 15) routinely exhibit a more pronounced biexponential kinetics. The faster component may be assigned to the Zn,Fe porphyrin, and the slower, of low amplitude (7% or 15%), can be attributed to an impurity or decomposition product. When the two chromophores are connected by the flexible propanediamine linker, dimer **12g** exhibits more complex kinetics that required a

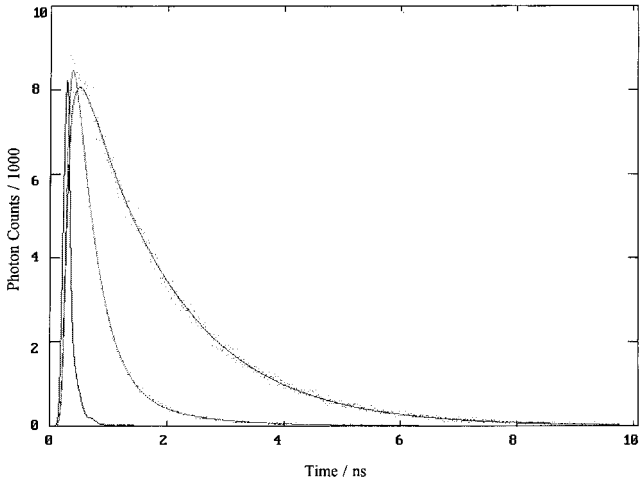

Figure 2. Typical 650-nm fluorescence decay curves for porphyrin dimers in dichloromethane. Dots are data points at 16.26-ps intervals; continuous lines are fits (which often overlay the dots). The curves are convoluted with the instrument response and are scaled by small factors for display on a common axis, in order of maxima from left to right: Instrument response function. **12c**: fit to 0.927 $\exp(-t/0.361\ \text{ns}) + 0.073\ \exp(-t/1.32\ \text{ns})$. **9c**: fit to 1.0 $\exp(-t/1.60\ \text{ns})$.

TABLE 1: Fluorescence Lifetimes of Monomeric and Dimeric Porphyrins in Dichloromethane

entry	compound[a]	structure	% fitting	τ, ns
1	H_2TPPF_5	**1**	100	9.1
2	$ZnTPPF_5$	**2**	99	1.68 ± 0.05
3	$Zn,Zn(TPPF_4)_2$-pip	**8a**	100	1.60 ± 0.05
4	$[Zn,Fe(TPPF_4)_2$-pip$]\cdot$OAc	**12a**	96[b]	0.070 ± 0.005
5	$[Zn,Fe(TPPF_4)_2$-pip$]\cdot$OAc[c]	**12a**	97[d]	0.107 ± 0.005
6	$Zn,Zn(TPPF_4)_2$-bcoda	**8b**	100	1.53 ± 0.02
7	$[Zn,Fe(TPPF_4)_2$-bcoda$]\cdot$OAc	**12b**	99	0.30 ± 0.02
8	$Zn,Zn(TPPF_4)_2$-bip	**8c**	100	1.60 ± 0.02
9	$[Zn,Fe(TPPF_4)_2$-bip$]\cdot$OAc	**12c**	93[e]	0.36 ± 0.02
10	$Zn,Zn(TPPF_4)_2$-stde	**8d**	99	1.57 ± 0.02
11	$[Zn,Fe(TPPF_4)_2$-stde$]\cdot$OAc	**12d**	98[f]	0.72 ± 0.02
12	$Zn,Zn(TPPF_4)_2$-stda	**8e**	99	1.59 ± 0.02
13	$[Zn,Fe(TPPF_4)_2$-stda$]\cdot$OAc	**12e**	99[g]	0.85 ± 0.02
14	$Zn,Zn(TPPF_4)_2$-pip-pfbp−pip	**8f**	100	1.59 ± 0.05
15	$[Zn,Fe(TPPF_4)_2$-pip-pfbp−pip$]\cdot$OAc	**12f**	85[h]	1.40 ± 0.05
16	$ZnTPPCl_6F_5$	**4**	98[f]	0.620 ± 0.04
17	$Zn,Zn(TPPCl_6F_4)_2$-dmdap	**8g**	99[g]	0.620 ± 0.04
18	$[Zn,Fe(TPPCl_6F_4)_2$-dmdap$]\cdot$OAc	**12g**	57[i]	0.34

[a] Abbreviations: pip = piperazyl; bcoda = bicyclo[2.2.2]octane-1,4-diamine; bip = bipiperidyl; dmdap = *N*,*N*′-dimethyl-1,3-diaminopropyl; pfbp = perfluorobiphenyl; stda = steroidal diamine (5α-androstanyl-3β,17β-diamine); stde = steroidal diether (5α-androstanyl 3α,17β-diether). [b] Also 2% each with $\tau = 0.35 \pm 0.07$ and 1.6 ± 0.1 ns. [c] Without 1-methylimidazole. [d] Also 3% with $\tau = 2$ ns. [e] Also 7% with $\tau = 1.32 \pm 0.02$ ns. [f] Also 2% with $\tau = 2$ ns. [g] Also 1% with $\tau = 2$ ns. [h] Also 15% with $\tau = 0.65 \pm 0.05$ ns. [i] Also 38% with $\tau = 0.105$ ns and 6% with $\tau = 0.96$ ns.

triexponential fit. This is probably a result of multiple conformations, each with its own distance and rate. This dimer is omitted from subsequent correlations, because its distance is not well-defined. In contrast, the monoexponential decay of the other dimers is evidence that their linkers are more rigid and impose a well-defined spatial relation between the two porphyrin rings. Even with the steroidal and bicyclooctane linkers, the possibility of conformational flexibility does not complicate the decay, so it is unlikely that the more pronounced biexponential kinetics in **12c** and **12f** is due to conformational heterogeneity, nor does the presence of regioisomers of **12e** (Table 1, entry 13) lead to discernible deviation from monoexponential kinetics, inasmuch as the distance between the two porphyrin rings is the same in both regioisomers. Therefore, our choice of edge-to-edge distance, rather than the more variable metal−metal distance, is justified, despite the possibility of internal rotations.

The measurements were generally conducted under conditions such that the acetate ligand on the iron was replaced in situ by two *N*-methylimidazoles. The Fe(III) acetate complex, with a high-spin iron located above the plane of the porphyrin, was thereby converted to an octahedral bis(imidazole)Fe(III) cationic complex with a low-spin iron in the porphyrin plane.[36] Table 1 shows that dimer **12a**, in the absence of 1-methylimidazole (entry 4), has a longer fluorescence lifetime than that in the presence of this ligand (entry 5). This result is consistent with faster ET to the low-spin planar six-coordinated bis(1-methylimidazole)iron(III) than to the high-spin five-coordinated iron(III) that is above the porphyrin plane.

The series of dimers **12a**−**g** represents a selection of linkers. The lifetimes in Table 1 generally increase with increasing length of the linker, from 0.1 and 0.3 ns for **12a** and **12b**, with one ring besides the C_6F_4 units, through 0.36 ns for **12c**, with two rings, to 0.72, 0.85, and 1.4 ns for **12d**, **12e**, and **12f**, with four rings. The three-fold through-bond pathway for electron transfer through the bicyclo[2.2.2]octane link of **12b** does not overcome the shorter distance in **12a**. The steroidal dimers **12d** and **12e** show quite similar lifetimes, indicating that there is no substantial difference between oxygen and nitrogen linkages of ether and amine.

Of particular interest is the comparison of the fluorescence lifetimes observed for the Zn,Fe heterodimers **12a**−**f** (Table 1) with those of the reference Zn,Zn homodimers **8a**−**f**. The lifetime of the homodimer provides the rate for all of the intrinsic deactivation processes in each skeleton under study. Actually there is little influence of the distant skeleton, because all of the $TPPF_4$ homodimers **8a**−**f** have nearly the same lifetime, which is quite close to that of the Zn monomer **2**, and dimer **8g** has the same lifetime as monomer **4**. The comparison of heterodimer with homodimer then provides a measure of ET, which represents the dominant fluorescence quenching mechanism.[16a,19] Moreover, the invariance of the observed rates to variation in dimer concentration from 10 to 100 μM excludes bimolecular contributions to the observed rates. Therefore, the deactivation of the photoexcited metalloporphyrin dimers can be analyzed using eqs 1−3 and converted to electron-transfer rate constants k_{ET}.

Distance Dependence of Electron-Transfer Rates. The electron-transfer rate constants k_{ET} for the Zn,Fe dimers **12a-f** are presented in Table 2, along with three different measures of the distances from porphyrin edge to porphyrin edge. For comparison, the dimers with polyphenylene and bicyclo[3.3.0]-octylidene spacers are also included. Direct donor−acceptor coupling is extremely weak at the long distances involved here. Therefore, the intervening bridge must mediate the donor−acceptor interaction.

It is interesting to compare all of the dimers with the same 13.9−14.4 Å edge-to-edge distance. The rate constant for ET in the piperazine-linked dimer **12a** is 18 times that of the dimer with a terphenylene spacer.[16a] Likewise, ET in **12a** is faster than that across the bicyclo[3.3.0]octylidene spacers.[19] This difference is perhaps due to the heterocyclic ring with nitrogen lone pairs in **12a** in place of the alkane, diene, and aromatic rings in the comparison dimers. However, another possible explanation is that electron transfer is faster in **12a** because it has a low-spin bis(imidazole)Fe(III) that is already in the porphyrin plane, as

TABLE 2: Electron-Transfer Rate Constants and Interporphyrin Distancesfor Dimeric Zn,Fe Porphyrins

structure	bridge[a]	d_{space}, Å	d_{bond}, Å	N_{bond}	τ, ns	10^{-9} k_{ET}, s^{-1}	decay per ring
	C_6H_4[b]	5.8	7.2	5	0.025	40[c]	
	$(C_6H_4)_2$[b]	10.1	12.9	9	0.15	6[c]	0.15
	$(C_6H_4)_3$[b]	14.4	18.6	13	0.90	0.8[c]	0.13
	C_6H_4-BCO-C_6H_4[d]	13.9		14		4.3	
	C_6H_4-BCOE-C_6H_4[d]	14.4		14		8.8	
12a	C_6F_4-pip-C_6F_4	14.4	18.6	13	0.07 ± 0.005	14 ± 0.1	
12b	C_6F_4-bcoda-C_6F_4	15.2	21.7	15	0.3 ± 0.02	3.0 ± 0.01	
12c	C_6F_4-bip-C_6F_4	18.6	24.7	17	0.36 ± 0.02	2.1 ± 0.01	0.15
12d	C_6F_4-stde-C_6F_4	20.6	29.3	20	0.72 ± 0.02	0.75 ± 0.03	
12e	C_6F_4-stda-C_6F_4	21.4	29.4	20	0.85 ± 0.02	0.54 ± 0.02	
12f	C_6F_4-pip-pfbp-pip-C_6F_4	27.3	35.6	25	1.40 ± 0.05	0.085 ± 0.03	0.20

[a] BCO = bicyclo[3.3.0]octanylidene, BCOE = bicyclo[3.3.0]octadienylidene; other abbreviations are as in Table 1. [b] Reference 16a. [c] Corrected by subtracting $1/\tau_0$. [d] Reference 19.

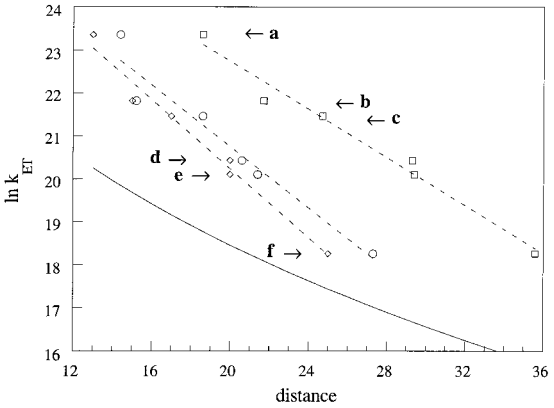

Figure 3. Distance dependence of ET rates in dimeric Zn,Fe porphyrins **12a**−**f**: d_{space} (○), d_{bond} (□), N_{bond} (◇), eq 5, with $R = d_{space} + 6.97$ Å (−).

compared to the bicyclo[3.3.0]octylidene dimer, where the Fe(III) was high-spin, five-coordinated, and above the porphyrin plane.

The long rigid saturated steroid skeleton of the stde and stda spacers in **12d** and **12e** represents an insulator between two tetrafluorophenyl rings. Yet electron transfer through these dimers is quite fast, not much slower than the other, previously measured dimers in Table 2, nor is there any deviation associated with the ether links unique to **10d**. Moreover, it is remarkable that electron transfer in **12f**, across the C_6F_4-pip-pfbp-pip-C_6F_4 spacer, is fast enough to be measured, albeit with a larger relative error than that for the shorter spacers. The through-space distance of 27.3 Å or the through-bond distance of 35.6 Å is quite long, especially for a saturated spacer, although it is not as long as the 40 Å across which an electron has been seen to travel from a guanine to an anthraquinone in duplex DNA, which is aromatic.[37]

The data in Table 2 show that there is a consistent decrease of the ET rate constant with increasing number of bonds, through-space distance, or through-bond distance. The matrix element governing ET can be assumed to decrease exponentially with distance,[38] resulting in a distance dependence for the rate that should follow eq 4, where k_0 is the limiting ET rate when the donor and acceptor are at the van der Waals contact distance r_0 and where β is the decay constant, also called the distance decay factor. The equation is so simple because matching the zinc porphyrin with the identical iron porphyrin maintains a constant energetic driving force.[1] Also, this equation incorporates into β any distance dependence of the solvent reorganization energy,[39] although this is likely to be negligible because the positive charges are delocalized over porphyrin rings. Figure 3 shows plots of ln k_{ET} vs these various distance measures. It is clear that eq 4 is followed well regardless of the particular choice of distance measure.

TABLE 3: Comparison of β Values for Electron Transfer Across Spacer Rings

ET system	distance	β, $Å^{-1}$	k_0, s^{-1}	correl coeff	$k(r)/k(r + 4$ Å$)$
polyphenylene spacers[a]	d_{space}	0.45	5.7×10^{11}	0.9998	6
	d_{bond}	0.34	4.8×10^{11}	0.9998	4
	N_{bond}	0.49[b]	4.7×10^{11}	0.9999	
12a−**f**	d_{space}	0.36	1.3×10^{12}	0.970	4
	d_{bond}	0.28	2.0×10^{12}	0.988	3
	N_{bond}	0.40[b]	1.9×10^{12}	0.989	

[a] Reference 16a, corrected with $1/\tau_0$. [b] Per bond.

$$k(r) = k_0 \exp[-\beta(r-r_0)] \quad (4)$$

The values of β and k_0 obtained from least-squares fitting of the data in Table 2 for each of the distance measures are summarized in Table 3. The scatter is greater, and the correlation coefficient is lower, than that seen with the polyphenylene series,[16a] which is also included. However, this latter is structurally homogeneous, whereas **12a**−**f** include a variety of intervening atoms. Moreover, k_0 near 2×10^{12} is in good agreement with that seen for electron transfer from a zinc porphyrin to a directly attached quinone.[40] The good linearity suggests that the current theory of electron tunneling via a nonconducting spacer ought to be applicable to all of these.

Previous studies of the distance dependence of PET rates in covalently linked systems have found that β lies between 0.5 and 1.5 $Å^{-1}$, with the smallest values for bridges involving mainly π orbitals.[9] Yet our value of 0.36 or 0.28 $Å^{-1}$, depending on the distance measure chosen, is considerably smaller than these and slightly smaller than the values for the phenylene spacers.[16a] Such low values mean that the ET rates are only weakly attenuated by increasing the length of the bridge.

Also included in Table 3 is $k(r)/k(r + 4$ Å$)$, which is the factor by which the rate is reduced on increasing the distance by 4 Å and which can be calculated as $\exp(4\beta)$. In previous cases this reduction factor was 20-fold[41] for aromatic spacers and 100-fold for aliphatic ones.[5b] The difference has been attributed to a superexchange mechanism that is more effective with the aromatic spacers. However, the five-fold reduction factor for the phenylene spacers, which are also aromatic, is significantly lower,[16a] and the reduction factor for dimers **12a**−**f**, which include both aromatic and aliphatic spacers, is even lower, only three- or four-fold. These comparisons imply that the aromatic nature of the spacer is not the only determinant of the distance dependence.

The weak attenuation of ET rates with increasing length of these aliphatic spacers is surprising. Perhaps electron transfer through the thick "wire" of the long steroidal bridges, which have more parallel pathways, competes adequately with the transfer through the thin "wire" of the aromatic bridges. However, that does not account for the rate with the C_6F_4-pip-pfbp-pip-C_6F_4 spacer. We conclude that electrons can find a path to tunnel through the σ bonds of saturated systems and that nitrogen or oxygen lone pairs facilitate this process.

The distance dependence of ET is regulated by coupling pathways that are optimal combinations of through-bond, through-space, and hydrogen-bond links, rather than simply depending on through-space distance.[3] As the tunneling electron propagates through a covalent bond, its wave function decays by a factor ϵ. For proteins an average ϵ was estimated as 0.6. Then the wave function decay per ring, with its two paths, is given by $2\epsilon^4$, and the rate decay per ring, which is proportional to the square of the wave function, is $4\epsilon^8$. The rate decays per ring for dimers **12c** and **12f** are included in Table 2, along with those for the phenylene spacers. From the average of these decays, a value of 0.67 is obtained, remarkably close to that in proteins.

Finally, it is necessary to demonstrate that these rates really do represent electron transfer, rather than energy transfer. Some experimental results and authorities are cited above,[19] including a transient absorption feature at 600−700 nm in similar Zn,Fe porphyrin dimers attributable to the Zn porphyrin cation,[16a] and that assignment was supported by the influence of solvent dynamics on electron transfer in cofacial porphyrin dimers.[42]

Yet the possibility of excitation energy transfer has not been rigorously excluded. We now estimate the rate of energy transfer by the Förster dipole−dipole mechanism, which is given by eq 5,[43] where τ_0 is the excited-state lifetime in the absence of energy

$$k_E = (1/\tau_0)(R_0/R)^6 \qquad (5)$$

transfer, R is the distance between donor and acceptor transition dipoles, and $R_0 = (9000K^2Q \ln 10/128\pi^5 n^4 N)\int(f_D(\nu)\,\epsilon_A(\nu)/\nu^4)\,d\nu$, where K^2 is an orientation factor between 0 and 1, Q is the donor fluorescence quantum yield in the absence of energy transfer, n is the refractive index of the medium, N is Avogadro's number, ν is frequency in cm^{-1}, $f_D(\nu)$ is the fluorescence spectrum of the donor normalized to unit area, and $\epsilon_A(\nu)$ is the decadic molar absorptivity of the acceptor in units of $M^{-1}\,cm^{-1}$, leading to $R_0 \sim 20$ Å. Using $\tau_0 = 1.6$ ns from Table 1 leads to the continuous line in Figure 3, plotted versus d_{space}, the difference between R and twice the distance from the porphyrin center to its edge (6.97 Å). It is evident that the Förster mechanism is not fast enough to explain the experimental data. Moreover, it does not account for the experimental linearity. Therefore, we conclude that eq 3 is indeed valid for the rate of electron transfer, but we cannot exclude a small contribution from energy transfer.[44]

Further effort will probe the dependence of PET rate on exergonicity. We are currently employing this sequential building-block approach to the synthesis of another series of metalloporphyrin dimers. It is thereby possible to introduce a variety of different substituents onto the acceptor porphyrin while maintaining a constant piperazine linker.

Conclusions

A series of metal *meso*-tetraarylmetalloporphyrin dimers have been synthesized. These dimers were designed to investigate critical geometric parameters governing ET rates. Synthetic methods for the preparation for these dimers are presented here. The rigid bridges allow the investigation of incremental distance effects on k_{ET} for similar collinear orientations, with edge-to-edge distances ranging from 14.4 to 27.3 Å. The precise control of the donor−acceptor separation distance allows unambiguous determination of ET rates from time-resolved fluorescence measurements. The rates obtained show a remarkably low falloff of rate with distance, even with the partly saturated linkages.

Acknowledgment. We thank José N. Onuchic for thoughtful discussions of bridge-mediated tunneling. This work was supported by the National Institutes of Health (Research Grant HL13581) and by Fundação de Amparo à Ciência e Tecnologia (Governo do Estado de Pernambuco, Recife, Brazil).

References and Notes

(1) Marcus, R. A.; Sutin, N. *Biochim. Biophys. Acta* **1985**, *811*, 265.

(2) Sutin, N. In *Electron Transfer in Inorganic, Organic, and Biological Systems*; Bolton, J. R., Mataga, N., McLendon, G., Eds.; Advances in Chemistry Series 228; American Chemical Society: Washington, DC, 1991; Chapter 3, p 25. Miller, J. R. In *Electron Transfer in Inorganic, Organic, and Biological Systems*; Bolton, J. R., Mataga, N., McLendon, G., Eds.; Advances in Chemistry Series 228; American Chemical Society: Washington, DC, 1991; Chapter 17, p 265. Gray, H. B.; Winkler, J. R. *Annu. Rev. Biochem.* **1996**, *65*, 537. Langen, R.; Chang, I. J.; Germanas, J. P.; Richards, J. H.; Winkler, J. R.; Gray, H. B. *Science* **1995**, *268*, 1733.

(3) Onuchic, J. N.; Beratan, D. N. *J. Am. Chem. Soc.* **1987**, *109*, 6771. Beratan, D. N.; Onuchic, J. N.; Winkler, J. R.; Gray, H. B. *Science* **1992**, *258*, 1740. Onuchic, J. N.; Beratan, D. N.; Winkler, J. R.; Gray, H. B. *Annu. Rev. Biophys. Biomol. Struct.* **1992**, *21*, 349−377. Beratan, D. N. *J. Am. Chem. Soc.* **1986**, *108*, 4321. Beratan, D. N.; Onuchic, J. N.; Betts, J. N.; Bowler, B. E.; Gray, H. B. *J. Am. Chem. Soc.* **1990**, *112*, 7915. Skourtis, S. S.; Regan, J. J.; Onuchic, J. N. *J. Phys. Chem.* **1994**, *98*, 3379.

(4) Turro, N. J.; Barton, J. K. *J. Biol. Inorg. Chem.* **1998**, *3*, 201. Lewis, F. D.; Letsinger, R. L. *J. Biol. Inorg. Chem.* **1998**, *3*, 215. Krider, E. S.; Meade, T. J. *J. Biol. Inorg. Chem.* **1998**, *3*, 222.

(5) (a) Joran, A. D.; Leland, B. A.; Felker, P. M.; Zewail, A. H.; Hopfield, J. J.; Dervan, P. B. *Nature* **1987**, *327*, 508. (b) Joran, A. D.; Leland, B. A.; Geller, G. G.; Hopfield, J. J.; Dervan, P. B. *J. Am. Chem. Soc.* **1984**, *106*, 6090. (c) Leland, B. A.; Joran, A. D.; Felker, P. M.; Hopfield, J. J.; Zewail, A. H.; Dervan, P. B. *J. Phys. Chem.* **1985**, *89*, 5571. (d) Khundkar, L. R.; Perry, J. W.; Hanson, J. E.; Dervan, P. B. *J. Am. Chem. Soc.* **1994**, *116*, 9700.

(6) McLendon, G. *Acc. Chem. Res.* **1988**, *21*, 160. Meyer, T. J. *Acc. Chem. Res.* **1989**, *22*, 163. Gust, D.; Moore, T. A. *Science* **1989**, *244*, 35. Gust, D.; Moore, T. A. *Top. Curr. Chem.* **1991**, *159*, 103. Macpherson, A. N.; et al. *J. Am. Chem. Soc.* **1995**, *117*, 7202.

(7) Connolly, J. S.; Bolton, J. R. In *Photoinduced Electron Transfer*; Fox, M. A., Chanon, M., Eds.; Elsevier: Amsterdam, The Netherlands, 1988; Chapter 6.2, Part A. Balzani, V.; Scandola, F. *Supramolecular Photochemistry*; Ellis Horwood: New York, 1991; pp 110−121 and references therein. Hayashi, T.; Ogoshi, H. *Chem. Soc. Rev.* **1997**, *26*, 355.

(8) Bowler, B. E.; Raphael, A. L.; Gray, H. B. *Prog. Inorg. Chem.* **1990**, *38*, 259. Winkler, J. R.; Gray, H. B. *Chem. Rev.* **1992**, *92*, 369. Mayo, S. L.; Ellis, W. R., Jr.; Crutchley, R. J.; Gray, H. B. *Science* **1986**, *233*, 948.

(9) Wasielewski, M. R. *Chem. Rev.* **1992**, *92*, 435. Sakata, Y.; Tsue, H.; O'Neil, M. P.; Wiederrecht, G. P.; Wasielewski, M. R. *J. Am. Chem. Soc.* **1994**, *116*, 6904.

(10) Osuka, A.; et al. *Bull. Chem. Soc. Jpn.* **1992**, *65*, 2807. Osuka, A.; Maruyama, K. *Pure Appl. Chem.* **1990**, *62*, 1511.

(11) Chambron, J. C.; Harriman, A.; Heitz, V.; Sauvage, J. P. *J. Am. Chem. Soc.* **1993**, *115*, 7419. Kurreck, H.; Huber, M. *Angew. Chem., Int. Ed. Engl.* **1995**, *34*, 849.

(12) Wynne, K.; Lecours, S. M.; Galli, C.; Therien, M. J.; Hochstrasser, R. M. *J. Am. Chem. Soc.* **1995**, *117*, 3749.

(13) Staab, H. A.; Hauck, R.; Popp, B. *Eur. J. Org. Chem.* **1998**, 631.

(14) Osuka, A.; Maruyama, K.; Mataga, N.; Asahi, T.; Yamakazi, I.; Tamai, N. *J. Am. Chem. Soc.* **1990**, *112*, 4958. Osuka, A.; Tanabe, N.; Kawabata, S.; Yamazaki, I.; Nishimura, Y. *J. Org. Chem.* **1995**, *60*, 7177.

(15) Berg, A.; Rachamim, M.; Galili, T.; Levanon, H. *J. Phys. Chem.* **1996**, *100*, 8791.

(16) (a) Helms, A.; Heiler, D.; McLendon, G. *J. Am. Chem. Soc.* **1992**, *114*, 6227. (b) Helms, A.; Heiler, D.; McLendon, G. *J. Am. Chem. Soc.* **1991**, *113*, 4325. (c) Heiler, D.; McLendon, G.; Rogalskyj, P. *J. Am. Chem. Soc.* **1987**, *109*, 604.

(17) Bolton, J. R.; et al. In *Electron Transfer in Inorganic, Organic, and Biological Systems*; Bolton, J. R., Mataga, N., McLendon, G., Eds.;

Advances in Chemistry Series 228; American Chemical Society: Washington, DC, 1991; Chapter 7, p 118. Newton, M. D. *Chem. Rev.* **1991**, *91*, 767.

(18) Sessler, J.; Johnson, M.; Liu, T.; Creager, S. J. *J. Am. Soc. Chem.* **1988**, *110*, 3659. Sessler, J. L.; Johnson, M. R.; Creager, S. E.; Fettinger, J. C.; Ibers, J. A. *J. Am. Chem. Soc.* **1990**, *112*, 9310. Sessler, J. L.; Johnson, M. R.; Lin, T.-Y. *Tetrahedron* **1989**, *45*, 4767. Rodriguez, J.; Kirmaier, C.; Johnson, M. R.; Friesner, R. A.; Holten, D.; Sessler, J. S. *J. Am. Chem. Soc.* **1991**, *113*, 1652.

(19) de Rege, P. J. F.; Williams, S. A.; Therien, M. J. *Science* **1995**, *269*, 1409.

(20) Battioni, P.; Brigaud, O.; Desvaux, H.; Traylor, T. G. *Tetrahedron Lett.* **1991**, *32*, 2893.

(21) Schmidt, J. A.; Liu, J. Y.; Bolton, J. R.; Archer, M. D.; Gadzekpo, V. P. Y. *J. Chem. Soc., Faraday Trans. 1* **1989**, *85*, 1027.

(22) Magde, D.; Campbell, B. F. *SPIE* **1989**, *1054*, 61.

(23) Assis, M. D.; Smith, J. R. L. *J. Chem. Soc., Perkin Trans. 2* **1998**, 2221. Magde, D.; Portela, C. F.; Richards, J. L.; Schöllhorn, B.; Traylor, T. G. 2nd European Bioinorganic Conference on Metal Ions in Biological Systems (EUROBIC II), Florence, Italy, 1994; Abstract 288.

(24) Smith, C. R. *J. Am. Chem. Soc.* **1928**, *50*, 1936.

(25) (a) Della, E. W.; Tsanaktsidis, J. *Aust. J. Chem.* **1985**, *38*, 1705. (b) Adcock, W.; et al. *J. Phys. Org. Chem.* **1991**, *4*, 353.

(26) Davis, M.; Parnell, E. W.; Rosenbaum, J. *J. Chem. Soc. C* **1967**, 1045.

(27) Wagner, R. W.; Johnson, T. E.; Li, F. R.; Lindsey, J. S. *J. Org. Chem.* **1995**, *60*, 5266. Lindsey, J. S.; Prathapan, S.; Johnson, T. E.; Wagner, R. W. *Tetrahedron* **1994**, *50*, 8941.

(28) Chang, C. K.; Abdalmuhdi, I. *J. Org. Chem.* **1983**, *48*, 5388. Chang, C. K.; Abdalmuhdi, I. *Angew. Chem., Int. Ed. Engl.* **1984**, *23*, 164. Eaton, S. S.; Eaton, G. R.; Chang, C. K. *J. Am. Chem. Soc.* **1985**, *107*, 3177. Fillers, J. P.; Ravichandran, K. G.; Abdalmuhdi, I.; Tulinsky, A.; Chang, C. K. *J. Am. Chem. Soc.* **1986**, *108*, 417.

(29) Collman, J. P.; et al. *J. Am. Chem. Soc.* **1992**, *114*, 9869. Guilard, R.; et al. *J. Am. Chem. Soc.* **1992**, *114*, 9877.

(30) Osuka, A.; Nakajima, S.; Maruyama, K. *J. Org. Chem.* **1992**, *57*, 7355. Osuka, A.; Kobayashi, F.; Nakajima, S.; Maruyama, K.; Yamazaki, I.; Nishimura, Y. *Chem. Lett.* **1993**, 161. Osuka, A.; Liu, B.-L.; Maruyama, K. *J. Org. Chem.* **1993**, *58*, 3582.

(31) Lindsey, J. S.; Schreiman, I. C.; Hsu, H. S.; Kearney, P. C.; Marguerettaz, A. M. *J. Org. Chem.* **1987**, *523*, 827. Lindsey, J. S.; Wagner, R. W. *J. Org. Chem.* **1989**, *54*, 829.

(32) van der Made, A. W.; Hoppenbrouwer, E. J. H.; Nolte, R. J. M.; Drenth, W. *Recl. Trav. Chim. Pays-Bas* **1988**, *107*, 15.

(33) Longo, F. R.; Finareli, M. G.; Kim, J. B. *J. Heterocycl. Chem.* **1968**, *6*, 927.

(34) Kobayashi, H. *Adv. Biophys.* **1975**, *8*, 191.

(35) Ruzicka, L.; Goldberg, M. W. *Helv. Chim. Acta* **1936**, *19*, 99.

(36) Scheidt, W. R.; Reed, C. A. *Chem. Rev.* **1981**, *81*, 543. Scheidt, W. R. In *The Porphyrins*; Dolphin, D., Ed.; Academic Press: New York, 1978; Vol. 3A, p 463. Collins, D. M.; Countryman, R.; Hoard, J. L. *J. Am. Chem. Soc.* **1972**, *94*, 2066.

(37) Gasper, S. M.; Schuster, G. B. *J. Am. Chem. Soc.* **1997**, *119*, 12762.

(38) Hopfield, J. J. *Proc. Natl. Acad. Sci. U.S.A.* **1974**, *71*, 3640.

(39) Isied, S. S.; Vassilian, A.; Wishart, J. F.; Creutz, C.; Schwarz, H. A.; Sutin, N. *J. Am. Chem. Soc.* **1988**, *110*, 635.

(40) Wynne, K.; LeCours, S. M.; Galli, C.; Therien, M. J.; Hochstrasser, R. M. *J. Am. Chem. Soc.* **1995**, *117*, 3749.

(41) Finckh, P.; Heitele, H.; Volk, M.; Michel-Beyerle, M. E. *J. Phys. Chem.* **1988**, *92*, 6584.

(42) Zaleski, J. M.; Chang, C. K.; Nocera, D. G. *J. Phys. Chem.* **1993**, *97*, 13206.

(43) Berlman, I. B. *Energy Transfer Parameters of Aromatic Compounds*; Academic Press: New York, 1973; pp 27 and 28.

(44) Yang, S. I.; Lammi, R. K.; Seth, J.; Riggs, J. A.; Arai, T.; Kim, D.; Bocian, D. F.; Holten, D.; Lindsey, J. S. *J. Phys. Chem.* **1998**, *102*, 9426.